Elimination of PknL and MSMEG_4242 in Mycobacterium smegmatis alters the character of the outer cell envelope and selects for mutations in Lsr2

Estalina Báez-Ramírez, Luis Querales, Carlos Andres Aranaga, Gustavo López, Elba Guerrero, Laurent Kremer, Séverine Carrère-Kremer, Albertus Viljoen, Mamadou Daffé, Françoise Laval, et al.

The Cell Surface 7 (2021) 100060

Contents lists available at ScienceDirect

The Cell Surface

journal homepage: www.sciencedirect.com/journal/the-cell-surface

Elimination of PknL and MSMEG_4242 in *Mycobacterium smegmatis* alters the character of the outer cell envelope and selects for mutations in Lsr2

Estalina Báez-Ramírez [a], Luis Querales [a], Carlos Andres Aranaga [a,1], Gustavo López [a,8], Elba Guerrero [a], Laurent Kremer [b,2], Séverine Carrère-Kremer [b,3], Albertus Viljoen [b,4], Mamadou Daffé [c], Françoise Laval [c], Stewart T. Cole [d,5], Andrej Benjak [d,6], Pedro Alzari [e], Gwenaëlle André-Leroux [e,7], William R. Jacobs Jr. [f], Catherine Vilcheze [f], Howard E. Takiff [a,g,*]

[a] *Laboratorio de Genétic Molecular, CMBC, Instituto Venezolano de Investigaciones Científicas (IVIC), Caracas, Venezuela*
[b] *Institut de Recherche en Infectiologie de Montpellier, Centre National de la Recherche Scientifique UMR 9004, Université de Montpellier, Montpellier, France*
[c] *Institut de Pharmacologie et de Biologie Structurale, Université de Toulouse, France*
[d] *EPFL, Lauzanne, Switzerland*
[e] *Unit of Structural Microbiology, Institut Pasteur, Paris, France*
[f] *Department of Microbiology and Immunology, Albert Einstein College of Medicine, Bronx, NY, USA*
[g] *Shenzhen Nanshan CCDC, 7 Huaming Road, Nanshan, Shenzhen, China*

ARTICLE INFO

Keywords:
Tuberculosis
Kinase
PknL
Lsr2
Biofilms
Mycobacterial envelope

ABSTRACT

Four serine/threonine kinases are present in all mycobacteria: PknA, PknB, PknG and PknL. PknA and PknB are essential for growth and replication, PknG regulates metabolism, but little is known about PknL. Inactivation of *pknL* and adjacent regulator *MSMEG_4242* in rough colony *M. smegmatis* mc^2155 produced both smooth and rough colonies. Upon restreaking rough colonies, smooth colonies appeared at a frequency of ~ 1/250. Smooth mutants did not form biofilms, showed increased sliding motility and anomalous lipids on thin-layer chromatography, identified by mass spectrometry as lipooligosaccharides and perhaps also glycopeptidolipids. RNA-seq and Sanger sequencing revealed that all smooth mutants had inactivated *lsr2* genes due to mutations and different IS*1096* insertions. When complemented with *lsr2*, the colonies became rough, anomalous lipids disappeared and sliding motility decreased. Smooth mutants showed increased expression of IS*1096* transposase TnpA and *MSMEG_4727*, which encodes a protein similar to PKS5. When *MSMEG_4727* was deleted, smooth *pknL/MSMEG_4242/lsr2* mutants reverted to rough, formed good biofilms, their motility decreased slightly and their anomalous lipids disappeared. Rough del*pknL/del4242* mutants formed poor biofilms and showed decreased, aberrant sliding motility and both phenotypes were complemented with the two deleted genes. Inactivation of *lsr2* changes colony morphology from rough to smooth, augments sliding motility and increases expression of *MSMEG_4727* and other enzymes synthesizing lipooligosaccharides, apparently preventing biofilm formation. Similar morphological phase changes occur in other mycobacteria, likely reflecting environmental adaptations. PknL and *MSMEG_4242* regulate lipid components of the outer cell envelope and their absence selects for *lsr2* inactivation. A regulatory, phosphorylation cascade model is proposed.

* Corresponding author at: Laboratorio de Genétic Molecular, CMBC, Instituto Venezolano de Investigaciones Científicas (IVIC), Caracas, Venezuela.
E-mail address: htakiff@gmail.com (H.E. Takiff).
[1] Current address: Facultad de Ciencias Básicas, Universidad Santiago de Cali, Cali, Colombia.
[2] INSERM, Institut de Recherche en Infectiologie de Montpellier, Montpellier, France.
[3] Current address : Institute of Regenerative Medicine and Biotherapies (IRMB), University of Montpellier, INSERM, Montpellier, France.
[4] Current address : Department for BioMedical Research, University of Bern, Switzerland.
[5] Current address : Institut Pasteur, Paris, France.
[6] Current address: Louvain Institute of Biomolecular Science and Technology, UCLouvain, Louvain-la-Neuve, Belgium.
[7] Current address: INRA, Unité MalAGE, Jouy-En-Josas, France.
[8] In memorium.

https://doi.org/10.1016/j.tcsw.2021.100060
Received 13 June 2021; Received in revised form 12 August 2021; Accepted 13 August 2021
Available online 25 August 2021

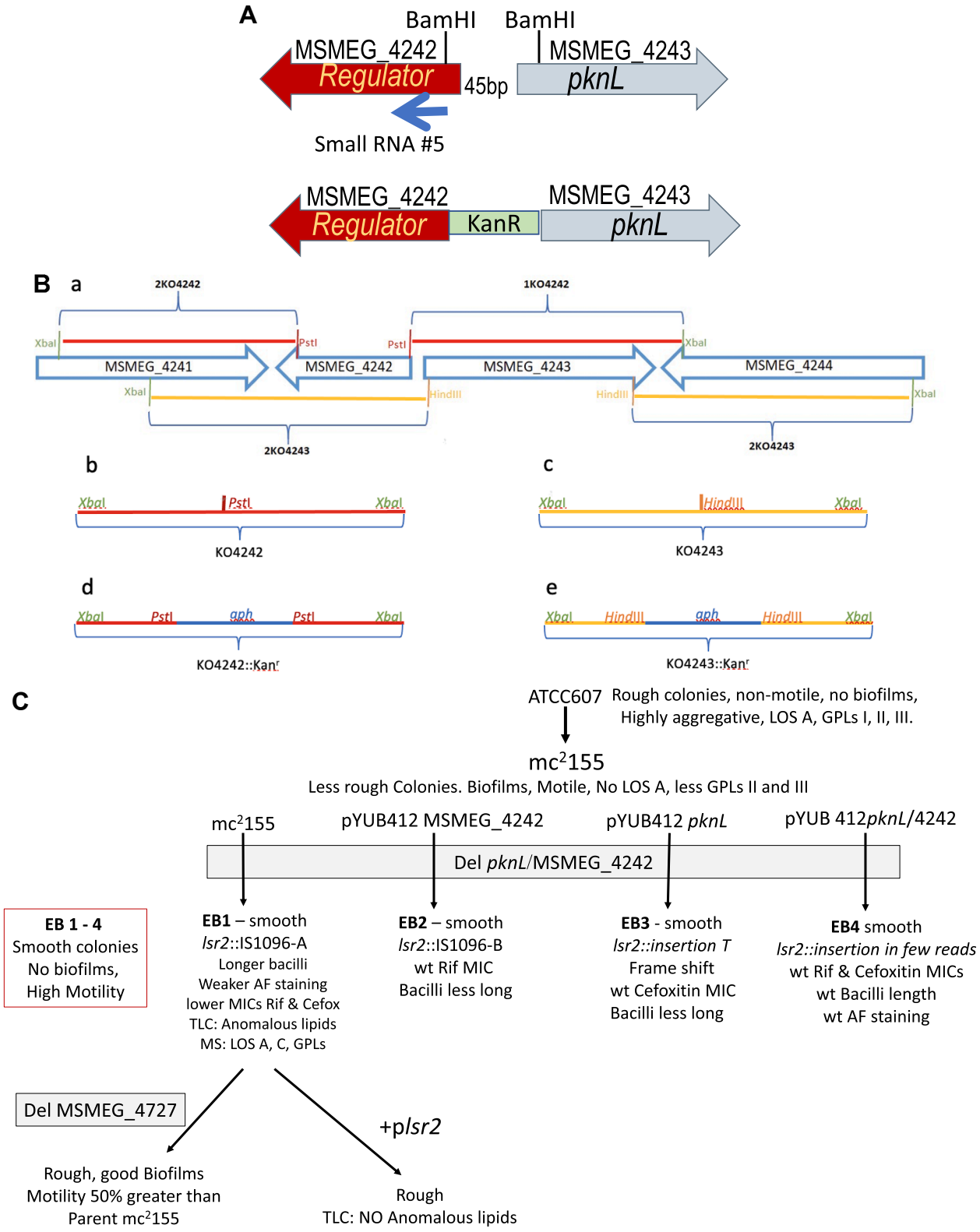

Fig. 1. **A.** Strategy for deleting both *MSMEG_4242* (a putative transcriptional regulator) and *MSMEG_4243* (*pknL*). A kanamycin resistance cassette replaced the 5′ terminal of both genes along with the intergenic region. This was inserted into plasmid pPR27, which carries a temperature sensitive mycobacterial origin of replication, the *sacB* gene and a gentamycin resistance cassette (Pelicic et al., 1997). **B.** Strategy for construction of strains lacking either *MSMEG_4242* or *MSMEG_4243* (*pknL*). **C.** Schematic diagram of strains originating from the first experiment to knock out both *MSMEG_4242* and *MSMEG_4243* (*pknL*) - EB1 – 4 and derivatives.**D.** Schematic diagram of strains originating from the second experiment to knock out both genes.

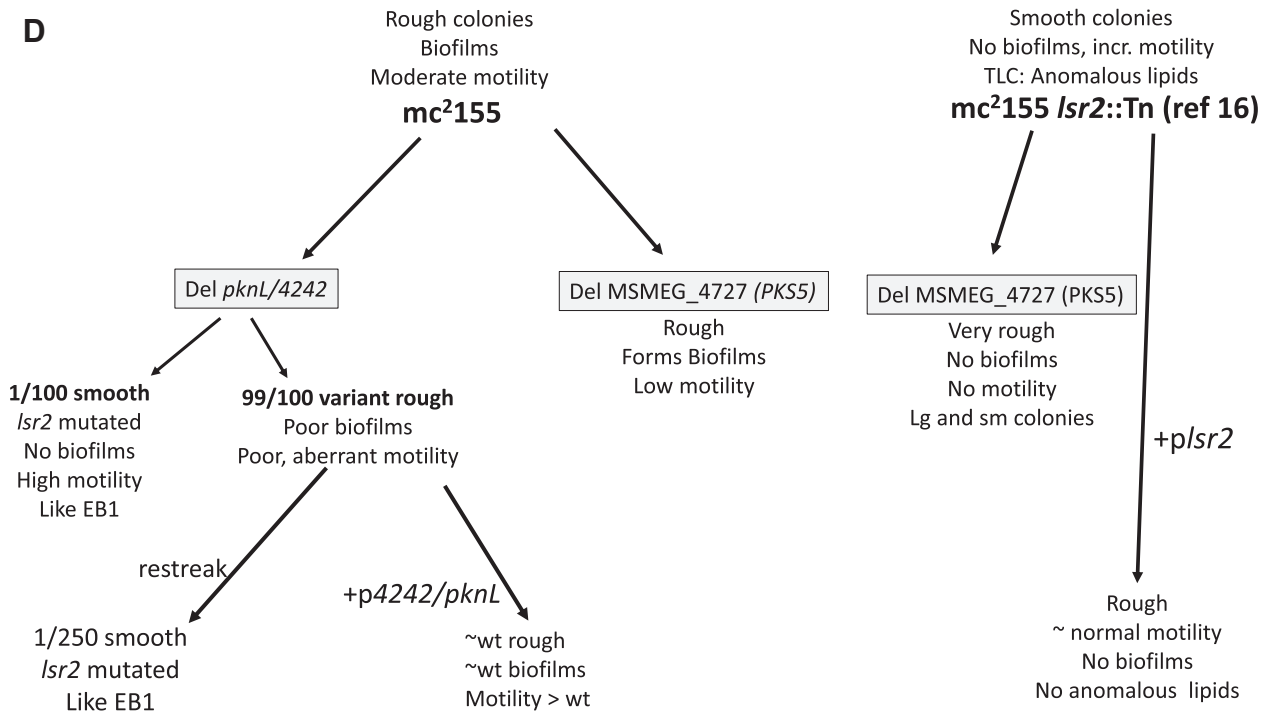

Fig. 1. (*continued*).

1. Introduction

Serine/threonine protein kinases (STPK) in mycobacteria appear to be involved in regulating cell growth, division and metabolism (Molle and Kremer, 2010). Of the 11 STK in *Mycobacterium tuberculosis*, only four are ubiquitous in mycobacterial species: PknA, PknB, PknG and PknL. Knockouts or overexpression of the essential PknA and PknB alter the shape of the bacilli, probably due to their involvement in the formation of the cell wall (Kang et al., 2005). Of the remaining 9 STK in *M. tuberculosis*, only PknL belongs to the same clade as PknA and PknB (Narayan et al., 2007; Wehenkel et al., 2008), but few studies have addressed its possible functions (Refaya et al., 2016) (Naz et al., 2021). PknL was shown to phosphorylate an adjacent and divergently transcribed, putative transcriptional regulator, Rv2175c (Canova et al., 2008; Cohen-Gonsaud et al., 2009), reducing its ability to bind DNA, but it is unknown what stimulates this phosphorylation, what genes Rv2175c regulates or what role PknL plays in the biology of the bacteria. This transcriptional regulator and the position of the gene encoding it are conserved in most mycobacteria.

Nine of the 11 STKs in *M. tuberculosis*, including PknA, PknB and PknL, contain transmembrane regions (Av-Gay and Everett, 2000). Based on the eukaryotic model for serine/threonine and tyrosine kinases, it is thought that the extracellular regions of the *M. tuberculosis* STPK may perceive a signal that activates the kinase regions within the bacteria. The extracellular region of PknB contains four PASTA (Penicillin-binding proteins And Serine/Threonine kinase Associated) (Bellinzoni et al., 2019) domains that are thought to interact with the peptidoglycan or its muropeptide precursors (Bellinzoni et al., 2019) to regulate PknB autophosphorylation. Mycobacterial PknL's have <10 extracellular amino acids beyond the transmembrane region, not enough for an extracellular receptor motif, and *Mycobacterium tuberculosis* PknL does not appear to be autophosphorylated but rather is phosphorylated by PknB and PknJ (Baer et al., 2014). However, the PknL in bacteria such as *Corynebacterium glutamicum* (Schultz et al., 2009) contain extracellular PASTA domains, suggesting that in these bacteria PknL could also be involved in regulating the synthesis of components of the cell wall or cell envelope.

To study the role of PknL in mycobacteria, we constructed strains of *Mycobacterium smegmatis* lacking functional copies of *pknL* (*MSMEG_4243*) and the adjacent putative transcriptional regulator *MSMEG_4242*, as well as knockout strains containing intact, complementing copies of one or both genes. Some of the knockout strains formed smooth colonies distinct from the rough colony parent *mc²155*. The strains were characterized for phenotypes associated with the cell envelope, their lipid composition and transcriptomes.

2. Results

2.1. Construction of ΔpknL/ΔMSMEG_4242 mutants and complementing phenotypes

The 5′ end encoding the N-terminal regions of the adjacent and divergently transcribed genes *pknL* and *MSMEG_4242* were replaced with a kanamycin resistance cassette (Fig. 1A). In a first experiment, the double mutant was constructed in the rough colony parental strain *M. smegmatis mc²155* as well as in strains containing integrating plasmid pYUB412int carrying either *pknL*, *MSMEG_4242*, or both genes (EB1 – 4, Fig. 1A & C,). Very few colonies were obtained, and all had a smooth morphotype (Fig. 2A). The deletion of both genes was initially confirmed by PCR amplification and restriction digests and subsequently by RNA-seq (data not shown). The mutant strains that contained plasmid pYUB412int with *pknL* and *MSMEG_4242*, separately or together, altered the morphology slightly, but the colonies remained smooth (Fig. 2A). The knockout experiment was repeated by another of the authors, using the same construct to eliminate both genes from the parent *mc²155*. In this second experiment many colonies were obtained, most of which were rough, but about 1/100 were smooth (Fig. 1D). Surprisingly, it was confirmed that the two genes had been eliminated in both smooth and rough colony morphotypes (data not shown). When the rough colony knock out strains were restreaked, smooth colonies appeared at a frequency of about 1/200 – 1/300 . In this second series of experiments, single knockouts of *pknL* and *MSMEG_4242* were also constructed (Fig. 2B). Most of them showed the same rough phenotype as the double mutants and smooth colonies spontaneously appeared at the same

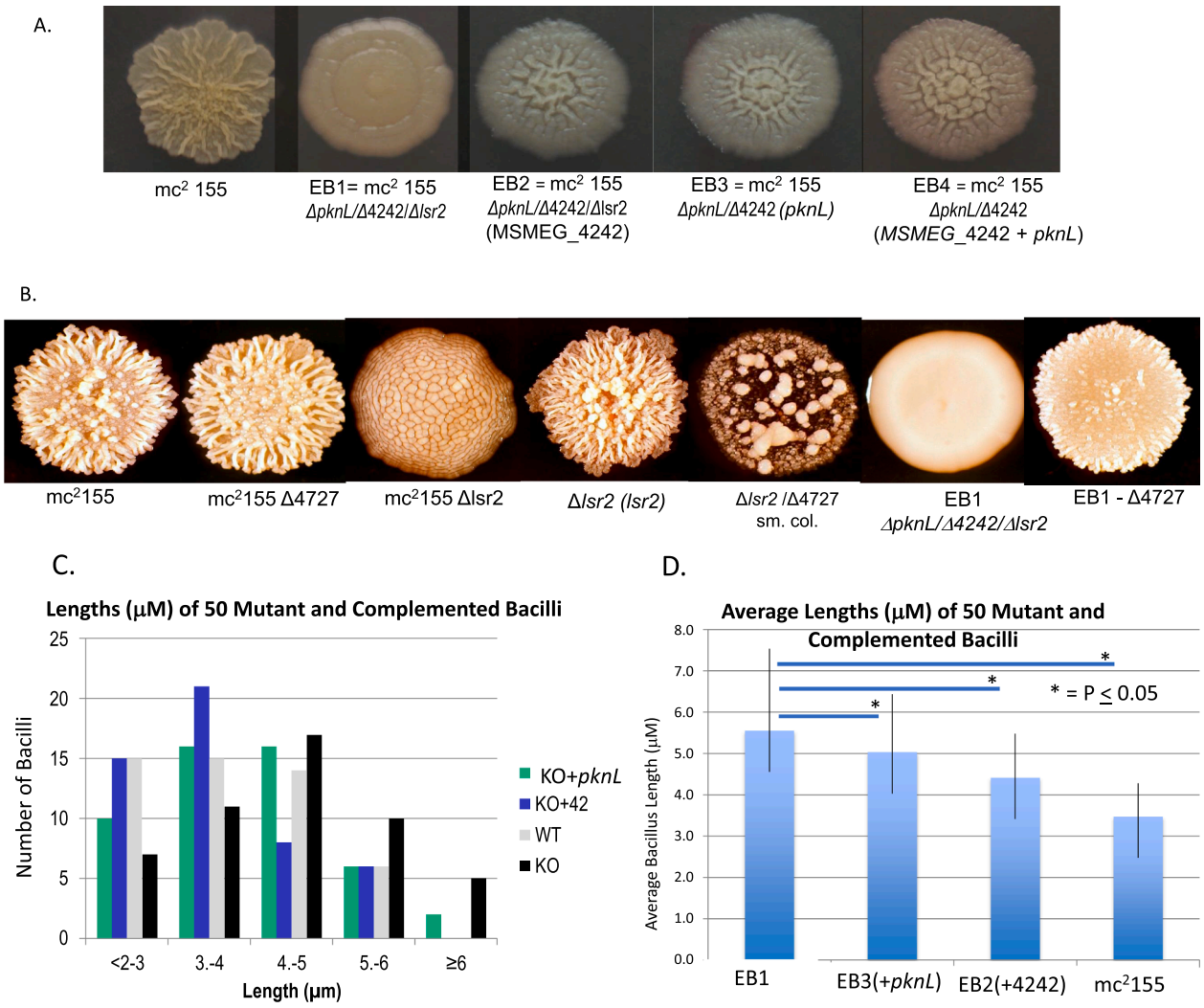

Fig. 2. .Fig. 2 Phenotypes of mutant strains. A. Colony Morphology of wt and mutant strains obtained in the first knockout experiment. B Colony Morphology of other strains in this study. C. Histogram showing measured length of 100 bacilli of each strain: wt, mc^{2}155; KO, EB1- mc^{2}155 Δ*pknL/*Δ*MSMEG_4242*; KO + 42, EB2 Δ*pknL/*Δ*MSMEG_4242* + pYUB412int*MSMEG_4242*; KO + *pknL*, EB3 Δ*pknL/*Δ*MSMEG_4242* + pYUB412int*pknL*.D.Histogram of the average lengths of 100 bacilli shown in C. Asterisk (*) indicates that the difference is statistically significant, P ≤ 0.05. E. Biofilms of the different strains, in duplicate. The +'s or –'s indicate the quality of the biofilm. F. Sliding motility of the different strains, in duplicate.

frequency as they arose in the double mutant strains. The single knockout strains were not studied further. Both genes were also inserted, separately, into expression vector pMV261 and the plasmids were transformed into mc^{2}155. The transformants showed no apparent alteration from the rough phenotype of the parent strain and were not studied further.

The smooth colony mutant strains were inoculated into liquid media and grew slightly, but not significantly slower than the *mc^{2}155* parent (data not shown). The uncomplemented smooth colony mutant EB1 (*mc^2*155 Δ*pknL/*Δ*MSMEG_4242*) also formed longer bacilli (Fig. 2C & D) and appeared to show weaker acid-fast staining (Suppl. Fig. S1). Complementation with *pknL* and *MSMEG_4242* restored both parental bacillus length and acid-fast staining. Strain EB1 was also two-fold more sensitive to rifampicin and cefoxitin than the parent mc^{2}155 (Table 1 and Fig. S2). The sensitivity to rifampicin was restored to that of the parent by complementation with just *pknL,* while complementation with both *pknL* and *MSMEG_4242* were required to regain parental cefoxitin sensitivity.

2.2. Altered biofilms and sliding motility

Smooth colony morphotypes have been associated with alterations in the lipid composition of the outer cell envelope (Kocíncová et al., 2008), so we examined two phenotypes associated with cell envelope lipids – sliding motility (Recht and Kolter, 2001) and biofilm formation (Kocíncová et al., 2008). While the rough colony parent mc^{2}155 forms strong biofilms and has moderate sliding motility, none of the smooth colony strains formed biofilms (Fig. 2E & 5), all had increased sliding motility (Fig. 2F & 5), and neither phenotype was restored to that of the parent by complementation with *pknL* and *MSMEG_4242* (Table 2).

In contrast, the sliding motility of the rough mc^{2}155 Δ*pknL/*Δ*MSMEG_4242* mutant was about half that of mc^{2}155 and was irregular and jagged, clearly different from the circular motility halos of all the other strains (Fig. 2F & 5). In addition, the rough Δ*pknL/*Δ*MSMEG_4242* mutants could form only very weak, delayed biofilms. When the rough Δ*pknL/*Δ*MSMEG*_4242 was complemented with a plasmid containing *pknL and MSMEG_4242*, the strain formed biofilms only slightly weaker than the unmutated mc^{2}155 parent and its sliding motility showed a

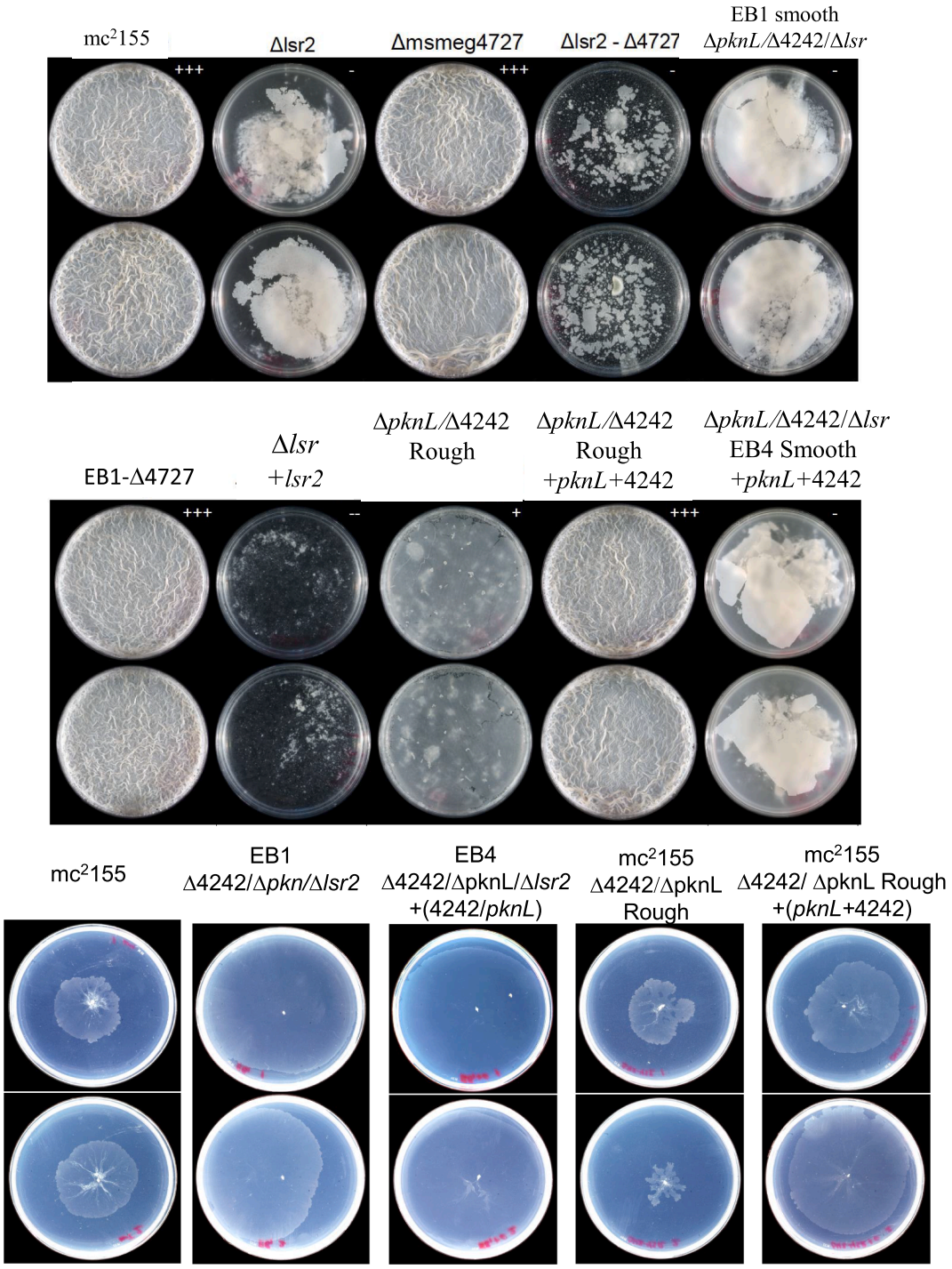

Fig. 2. (*continued*).

regular halo larger than that of the parent (Fig. 2E, 2F & 5 and Table 2). Thus, while the reduced motility and poor biofilms in the rough colony mutants were attributable to the absence of *pknL* and *MSMEG_4242*, the increased motility and lack of biofilms in the smooth mutants was not reversed by intact copies of these two genes.

2.3. Mutations in lsr2 were responsible for the smooth colony phenotype

RNA-seq of the smooth colony mutants (EB1-4) revealed that all contained mutations that inactivated the *lsr2* gene (*MSMEG_6092*) (Chen et al., 2008; Gordon et al., 2010). EB1 (Δ*pknL*/ΔMSMEG_4242) had a new IS1096 insertion into *lsr2*, while EB2 (Δ*pknL*/Δ4242-*MSMEG_4242*) had a different new IS1096 insertion into the *lsr2* gene. RNA-seq showed an increase in the expression of IS1096 transposase *tnpA* from some of the IS1096 insertions in EB1 and EB2 (Table 3). Strain EB3 (Δ*pknL*/Δ4242-*pknL*) had a one base, frameshifting insertion into *lsr2* (Fig. 3), while strain EB4 (*ΔpknL/ΔMSMEG_4242 – pknL/MSMEG_4242*), showed the same frameshifting but only in a minority of RNA-seq reads. This frameshifting mutation was also present in a small minority of reads from wt parent mc²155 and was seen in three reads from double knockout strain EB1. With successive passaging and restreaking, strain EB4 eventually reverted to a rough colony

Table 1
Sensitivity of mutants and complemented mutants to Rifampicin and Cefoxitin.

	Rifampicin 32 ug/ml	Rifampicin 64 ug/ml	Cefoxitin 12.5 ug/ml	Cefoxitin 25 ug/ml
mc^{2}155	++	++	++	++
Del *pknL/4242/lsr2 smooth*	++	–	++	–
Del *pknL/4242/lsr2 smooth* (4242)	++	–	++	+
Del *pknL/4242/lsr2 smooth* (pknL)	++	++	++	–
Del *pknL/4242/lsr2 smooth* (pknL/4242)	++	++	++	++
Del *lsr2*	++	+		
Del *lsr2* (*lsr2*)	++	++		
Del *pknL/4242* rough	++	++		
Del *pknL/4242* rough (*pknL/4242)*	++	++		

morphology. RNA-seq also showed increased expression of the IS1096 transposase *tnpA* from some of the other IS1096 insertions in EB1 and EB2 (Table 3), but no other new IS1096 insertions were found.

PCR amplification and Sanger sequencing showed that all smooth colony mutants isolated in the second knockout experiment, or smooth colonies that appeared spontaneously on restreaking these rough colony double mutants, also contained mutated *lsr2* genes, including IS*1096* insertions, a frameshift due to a nucleotide deletion and a mutation substituting an alanine for an aspartic acid at amino acid 35 (D35A) (Fig. S4). In contrast, the *lsr2* genes were intact in all rough colony mutants. When strain EB1 (*ΔpknL/ΔMSMEG_4242/Δlsr2)* was transformed with a plasmid carrying an intact copy of *lsr2*, the colony morphology reverted to rough.

2.4. Analysis of cell envelope lipids

Thin-layer chromatography (TLC) of smooth colony strain EB1 showed anomalous bands, predominantly in the polar fraction, that disappeared when the strain was transformed with a plasmid carrying *lsr2* and became rough (Fig. 4A & B.). These anomalous bands were not present on TLC of the rough colony *ΔpknL/ΔMSMEG_4242* strains.

Mass spectrometry (MS) of cell wall lipids of the uncomplemented smooth colony mutant EB1 revealed anomalous peaks that were not present in parent strain mc^{2}155 (Fig. 4C & D). The mass range of the peaks suggested that they were likely lipooligosaccharides A (LOS A) and C (LOS C) (Etienne et al., 2005), but there were also anomalous peaks in the size range of glycopeptidolipids (GPLs) (Etienne et al., 2005).

2.5. Elimination of MSMEG_4727 restored rough colony morphology in strain EB1.

The RNA-seq study of smooth colonies EB1 – EB3 also showed a marked increase in the transcripts of *MSMEG_4727* and other downstream genes implicated in the synthesis of LOS (Table 3) (Etienne et al., 2009; Colangeli et al., 2007). *MSMEG_4727* encodes a polyketide synthase similar to the PKS5 associated with the production of LOS in smooth colony *Mycobacterium canetti*. It was shown to be inactivated in rough colony *M. canetti* strains and *M. tuberculosis* (Boritsch et al., 2016). When the MSMEG_4727 gene was eliminated in strain EB1 to create EB1- *Δ4727 (ΔpknL/Δ4242/Δlsr2/Δ4727),* the colony morphology reverted to rough, although slightly different from the parent *mc^{2}155* (Figs. 5 and S3). The EB1-*Δ4727* strain was capable of forming normal biofilms and its sliding motility was reduced but still about 50% greater than that of parent *mc^{2}155* (Fig. 2E, 2F, 5 and Table 2). *W*hen MSMEG_4727 was eliminated from parent strain *mc^{2}155*, the resulting mutant could form normal biofilms but the sliding motility was reduced by nearly half. In contrast, when *MSMEG_4727* was deleted from an *lsr2 mutant* obtained by transposon mutagenesis of *mc^{2}155* strain NJS20 (Colangeli et al., 2007)*;* there was no motility and the strain could not form biofilms (Kocíncová et al., 2008). These results confirm that the inactivation of *lsr2* in the smooth colony *pknL*/4242 mutants led to increased production of LOS from the *MSMEG_4727* synthesis pathway, which prevented the formation of biofilms but contributed to motility.

3. Discussion

This study was undertaken to explore the role of PknL in mycobacterial biology but led to unexpected results. All smooth colony *pknL/MSMEG_4242* knockout strains harbored *lsr2* genes that had been mutated by frameshifts, amino acid substitutions or *IS1096* insertions, perhaps associated with the increased transcription of transposase TnpA seen on RNA-seq. The smooth mutants had two sets of phenotypes – those stemming from the lack of *PknL/MSMEG_4242* and those caused by absence of Lsr2. The phenotypes of the smooth triple mutant smooth EB1 strain (*ΔpknL/ΔMSMEG_4242/Δlsr2)* that were reversed with a plasmid carrying *pknL/MSMEG_4242* were: longer bacilli; poor acid-fast staining; and increased sensitivity to rifampicin and cefoxitin (Table 1 & Fig. S2). The phenotypes complemented by intact copies of *lsr2* included the smooth colony morphology, the inability to form biofilms, increased sliding motility and additional lipid species, probably LOS-A, LOS-C and subfamilies of GPL (Etienne et al., 2005). These are reminiscent of the phenotypes of the original *M. smegmatis* strain ATCC607 that were lost

Table 2
Phenotypes of parent and mutant strains.

	pknL/4242	*lsr2*	4727	Biofilm	Motility (in mm*)	Morphology
A: mc^{2}155	Yes	Yes	Yes	+++	38	rough
D: EB1	No	No	Yes	-	65	smooth
E: EB1 + p4242/4243	yes	No	Yes	-	68	smooth
I: EB1-Δ4727	No	No	No	+++	55	rough
H: mc^{2}155 Δ4727	Yes	Yes	No	+++	20	rough
F: Δ4242/4243(R)	No	Yes	Yes	+	20#	rough but altered
G: Δ4242/4243 + p4242/4243	yes	Yes	Yes	++	50	rough
B: Δ*lsr2*	Yes	No	Yes	- -	48	smooth
C: Δlsr2 + p*lsr2*	Yes	yes	Yes	- -	28	rough
J: Δ*lsr2*-Δ4727	Yes	No	No	-	4	very rough

*, Motility measured as millimeters of halo diameter.
#, irregular halo.
+++ Mature floating biofilm.
++ Mature biofilm.
+ Slow formation of biofilm.
- Abnormal biofilm.
- - No biofilm.

when it evolved into variant mc^{2}155(Etienne et al., 2005). Eliminating the PKS enzyme *MSMEG_4727* in EB1(mc^{2}155 Δ*pknL*/Δ*MSMEG_*4242/Δ*lsr2*) reversed the smooth colony morphotype and reduced motility, but when the single *lsr2* mutant was complemented with *lsr2,* it still could not form biofilms. This single *lsr2* mutant strain was obtained from another lab (Colangeli et al., 2007) and may have acquired additional genetic changes, which appear to be frequent in *M. smegmatis* strains (Kocíncová et al., 2008; Etienne et al., 2005).

To fit these results into a regulatory model, we compared our findings with previously published studies. PknL was shown to be incapable of autophosphorylation but was phosphorylated by PknB and PknJ and colocalized with PknB to the bacillus poles and midplane septa (Baer et al., 2014), sites thought to be related to bacterial replication. A recent study found that a strain of *M. tuberculosis* lacking PknL showed decreased survival in macrophages and the spleens of infected mice, and also showed increased Minimum Inhibitory Concentrations (MICs) for isoniazid and ethambutol (Naz et al., 2021). We found no difference in resistance to isoniazid, but a two-fold increase in susceptibility to rifampicin and cefoxitin. These are large molecules, so changes in their susceptibility could reflect changes in cell wall permeability(Kolodziej et al., 2021). It was reported that the absence of Lsr2 in *M. smegmatis* increases susceptibility to rifampicin and nalidixic acid(Kolodziej et al., 2021), and that overexpression of PknB increased susceptibility to rifampicin and vancomycin(Le et al., 2020) likely due to alterations of the cell envelope. Zeng et al. found that depletion of either PknA or PknB from *M. tuberculosis* reduced the MICs for cephalosporins, carbapenems and rifampicin (Zeng et al., 2020). We found that a strain with a mutated *lsr2* had increased susceptibility to rifampicin that was complemented with a parental copy of *lsr2* (Table 1). However, there was a greater increase in susceptibility in smooth strains lacking PknL and MSMEG_4242 in addition to Lsr2, and the rifampicin susceptibility returned to that of the parent when these strains were complemented only with *pknL* and *MSMEG_4242* (Table 1 and Suppl. Fig. 2). The lack of an increase in susceptibility in the rough Δ*pknL/ΔMSMEG_4242* mutants suggests that the deletion of PknL and *MSMEG_4242* has a synergistic effect with Lsr2 mutations in altering the cell envelope. It has been reported that Lsr2 also controls pigment in *M. smegmatis* (Kocíncová et al., 2008); but although some of the mutant strains had altered pigmentation, we did not analyze this phenotype.

In a study in *M. tuberculosis* using an antisense strategy, a strain with a PknL knockdown showed no change in colony morphology but, similar to our results, the mutant bacilli grew slower and were ~0.8 μm longer. They also found that the knockdown strain had lower viability over time but increased resistance to pH 5.5, SDS and lysozyme (Refaya et al., 2016). In contrast, a very recent study described shorter and wider bacilli in an *lsr2* mutant strain(Kolodziej et al., 2021).

Several publications have addressed Lsr2, a nucleoid-associated protein that has been associated with cell cycle(Kolodziej et al., 2021) and is essential in *M. tuberculosis* (Colangeli et al., 2007; Kolodziej et al., 2021; Kolodziej et al., 2021) (Chen et al., 2008; Gordon et al., 2010) but

Table 3
RNA-seq results of strains EB1, EB2 and EB3 vs EB4 and/or wt mc^{2}155

	EB1+2+3 vs. EB4+WT				EB1 vs. WT	EB2 vs. WT	EB3 vs. WT	
gene	foldChange	log2FC	pval	padj	log2FC	log2FC	log2FC	product
MSMEG_1128	90.83	6.51	0.00	0.00	6.22	5.83	4.49	hypothetical protein
MSMEG_1241	53.87	5.75	0.00	0.00	7.16	7.35	6.09	phospholipase D domain-containing protein
MSMEG_1129	34.45	5.11	0.00	0.00	4.41	4.35	4.31	D-amino-acid dehydrogenase
MSMEG_1240	27.65	4.79	0.00	0.00	5.15	5.48	4.69	Hist.kinase-like ATPase domain-containing protein
MSMEG_6147	18.63	4.22	0.00	0.00	5.06	5.12	4.42	hypothetical protein
MSMEG_3374	18.53	4.21	0.00	0.00	4.30	4.82	4.55	DUF2236 domain-containing protein
MSMEG_5461	15.72	3.97	0.00	0.00	4.01	4.10	3.38	hypothetical protein
MSMEG_1248	12.41	3.63	0.00	0.25	4.05	4.65	2.85	hypothetical protein
MSMEG_5708	11.23	3.49	0.00	0.00	3.98	4.10	3.70	DUF2510 domain-containing protein
MSMEG_5709	11.23	3.49	0.00	0.00	4.13	3.90	3.97	hypothetical protein
MSMEG_5972	10.69	3.42	0.00	0.00	3.36	3.29	3.09	hypothetical protein
MSMEG_4732	9.41	3.23	0.01	1.00	3.65	2.83	1.85	**glycosyl transferase family protein**
MSMEG_4729	9.10	3.19	0.00	0.39	3.36	2.91	1.74	**hypothetical protein**
MSMEG_1135	8.98	3.17	0.00	0.04	3.37	3.09	3.40	hypothetical protein
MSMEG_4728	8.73	3.13	0.00	0.25	3.73	2.95	2.40	**condensation domain-containing protein**
MSMEG_5460	8.43	3.08	0.00	0.00	2.53	3.07	2.65	hypothetical protein
MSMEG_5874	8.39	3.07	0.38	1.00	-0.87	4.70	1.07	tRNA-Thr
MSMEG_3429	8.31	3.06	0.01	0.74	3.87	3.89	1.91	O-acyl transferase
MSMEG_6579	8.03	3.01	0.00	0.02	1.99	3.13	2.84	MHB domain-containing protein
MSMEG_5710	7.99	3.00	0.00	0.00	3.96	4.14	3.83	EspA_EspE domain-containing protein
MSMEG_4727	7.89	2.98	0.00	0.00	3.30	2.90	2.34	**mycocerosic acid synthase**
MSMEG_2822	7.82	2.97	0.00	0.00	3.15	3.23	3.10	transposase, truncation
MSMEG_4242	7.81	2.96	0.00	0.01	2.52	2.86	2.60	transcriptional regulatory protein
MSMEG_5957	7.69	2.94	0.00	0.13	3.17	3.13	1.85	GDP-mannose 6-dehydrogenase AlgD
MSMEG_4730	7.55	2.92	0.01	1.00	2.93	2.44	1.20	**hypothetical protein**
MSMEG_1247	7.03	2.81	0.00	0.00	3.85	3.50	3.42	hypothetical protein
MSMEG_1238	6.80	2.76	0.00	0.07	3.13	3.50	2.23	type III restriction enzyme, res subunit
MSMEG_4706	6.73	2.75	0.35	1.00	0.42	3.50	0.06	tRNA-Arg
MSMEG_4731	6.68	2.74	0.00	0.42	2.93	2.14	1.71	**acyl-CoA synthetase**
MSMEG_1747	6.66	2.73	0.50	1.00	1.31	0.72	4.70	RNA polymerase sigma-70 factor
MSMEG_3564	6.49	2.70	0.00	0.01	2.65	3.30	2.35	bacterioferritin
MSMEG_4676	6.47	2.69	0.50	1.00	-2.27	3.69	-0.95	tRNA-Gly

(*continued on next page*)

Table 3 (*continued*)

MSMEG_2826	6.44	2.69	0.00	0.52	3.53	3.40	1.86	PIN_8 domain-containing protein
MSMEG_5758	6.35	2.67	0.41	1.00	-1.39	4.14	0.77	tRNA-Lys
MSMEG_1223	6.18	2.63	0.00	0.01	4.78	4.43	4.52	hypothetical protein
MSMEG_4478	6.11	2.61	0.44	1.00	-1.06	3.70	0.07	tRNA-Asn
MSMEG_1253	5.94	2.57	0.00	0.34	3.14	2.86	1.70	hypothetical protein
MSMEG_3579	5.79	2.53	0.00	0.13	3.65	3.05	2.48	transmembrane protein
MSMEG_5459	5.67	2.50	0.00	0.56	2.10	1.74	1.97	hypothetical protein
MSMEG_5092	5.64	2.50	0.02	1.00	2.75	3.28	1.29	hypothetical protein
MSMEG_5135	5.55	2.47	0.00	0.08	2.68	2.21	2.02	hypothetical protein
MSMEG_5535	5.44	2.44	0.09	1.00	3.36	2.49	0.48	hypothetical protein
MSMEG_0677	5.36	2.42	0.42	1.00	-1.89	3.58	0.70	tRNA-Gly
MSMEG_5090	5.36	2.42	0.00	0.13	3.11	2.72	1.92	hypothetical protein
MSMEG_1337	5.34	2.42	0.41	1.00	-1.14	3.87	0.78	tRNA-Thr
MSMEG_2149	5.32	2.41	0.00	0.02	3.42	3.11	2.53	hypothetical protein
MSMEG_3163	5.30	2.41	0.00	0.08	3.68	2.97	2.72	gp55 protein
MSMEG_5958	5.12	2.36	0.00	0.31	2.83	3.14	2.66	hypothetical protein
MSMEG_1868	5.09	2.35	0.01	1.00	2.87	2.60	1.10	hypothetical protein
MSMEG_2199	5.09	2.35	0.00	0.33	3.26	2.50	2.14	hypothetical protein
MSMEG_5558	5.06	2.34	0.04	1.00	2.44	2.46	3.82	hypothetical protein
MSMEG_3164	5.05	2.34	0.00	0.03	2.99	3.07	2.32	hypothetical protein
MSMEG_4746	5.04	2.33	0.50	1.00	-5.30	3.30	0.01	tRNA-Lys
MSMEG_2833	4.96	2.31	0.45	1.00	-1.21	3.31	0.00	tRNA-Val
MSMEG_3578	4.95	2.31	0.00	0.08	2.84	2.39	1.99	cyclase
MSMEG_5091	4.94	2.30	0.00	0.41	2.80	2.68	1.44	hypothetical protein
MSMEG_3577	4.93	2.30	0.00	0.21	2.05	2.08	1.70	calpastatin
MSMEG_5960	4.92	2.30	0.00	0.34	2.47	2.56	1.76	O-antigen polymerase
MSMEG_0828	4.80	2.26	0.00	0.13	2.20	2.25	2.62	immunogenic protein MPT63
MSMEG_1404	4.73	2.24	0.03	1.00	3.29	2.15	1.86	**IS1096, tnpA protein**
MSMEG_1746	4.72	2.24	0.55	1.00	0.68	0.51	3.90	6-hydroxy-D-nicotine oxidase
MSMEG_1965	4.70	2.23	0.45	1.00	-3.34	3.42	0.67	tRNA-Met
MSMEG_0384	4.63	2.21	0.00	0.09	3.37	2.79	2.37	glucose-1-phosphate thymidylyltransferase
MSMEG_3755	4.59	2.20	0.37	1.00	0.30	3.55	0.33	5S ribosomal RNA
MSMEG_1312	4.49	2.17	0.02	1.00	2.03	2.51	0.85	DUF2510 domain-containing protein
MSMEG_5134	4.48	2.16	0.00	0.39	1.65	2.02	1.14	hypothetical protein
MSMEG_5133	4.42	2.15	0.08	1.00	0.99	2.43	0.93	hypothetical protein
MSMEG_2836	4.34	2.12	0.49	1.00	-5.94	3.34	0.21	tRNA-Val
MSMEG_0200	4.32	2.11	0.02	1.00	2.84	2.96	1.18	hypothetical protein
MSMEG_2570	4.17	2.06	0.01	1.00	1.73	1.10	1.92	xanthine/uracil permease
MSMEG_6580	4.14	2.05	0.00	0.53	1.93	1.52	2.59	transcriptional regulator family protein
MSMEG_5425	4.03	2.01	0.36	1.00	0.32	3.48	0.65	tRNA-Gln
MSMEG_3955	0.23	-2.10	0.27	1.00	-0.46	0.17	0.18	Nitroreductase domain-containing protein
MSMEG_0621	0.23	-2.12	0.21	1.00	0.21	-1.08	-0.43	low molecular weight protein antigen 7
MSMEG_3951	0.22	-2.16	0.29	1.00	-1.71	0.46	1.19	hypothetical protein
MSMEG_0522	0.22	-2.21	0.19	1.00	-3.71	-2.99	-2.80	pp24 protein
MSMEG_3937	0.21	-2.25	0.31	1.00	-0.87	0.89	1.59	Urease subunit alpha
MSMEG_3946	0.21	-2.29	0.17	1.00	-2.24	-0.84	0.57	transmembrane protein
MSMEG_3929	0.20	-2.32	0.27	1.00	-1.38	-0.16	2.95	[NiFe] hydrogenase subunit delta
MSMEG_3954	0.18	-2.44	0.28	1.00	0.32	0.52	1.34	trehalose 6-phosphate phosphorylase
MSMEG_3930	0.18	-2.47	0.27	1.00	-0.53	0.32	2.32	[NiFe] hydrogenase subunit gamma
MSMEG_3931	0.15	-2.70	0.24	1.00	-1.06	0.09	2.21	[NiFe] hydrogenase subunit beta
MSMEG_3936	0.15	-2.74	0.24	1.00	-0.38	0.26	1.39	universal stress protein family protein
MSMEG_3953	0.14	-2.84	0.23	1.00	-2.33	0.31	1.51	hypothetical protein
MSMEG_3939	0.14	-2.88	0.27	1.00	0.17	0.85	0.53	universal stress protein family protein
MSMEG_3932	0.14	-2.88	0.22	1.00	-1.10	0.09	1.68	14 kDa antigen
MSMEG_3940	0.11	-3.16	0.22	1.00	-0.83	0.31	0.57	universal stress protein family protein
MSMEG_3934	0.10	-3.39	0.18	1.00	-1.44	-0.41	0.77	phosphoenolpyruvate synthase

not in *M. smegmatis*. The genes that Lsr2 appears to regulate – its regulon, is broad and overlaps with the PknB regulon (Alqaseer et al., 2019). It was previously observed that smooth colonies of *M. smegmatis* appear as spontaneous variants of *M. smegmatis* ATCC607, the parent strain of mc^2155, as a result of insertions of IS*1096* into *lsr2* (Kocíncová et al., 2008). These hypermotile variants, which are unable to form biofilms, appeared in a starvation experiment with a *relA* (stringent response) mutant at a frequency of approximately 10^{-4} (Arora et al., 2008), higher than the expected frequency of about 10^{-6}. In our rough colony *pknL/MSMEG_4242* knockout mutants, the insertions, deletions, amino acid

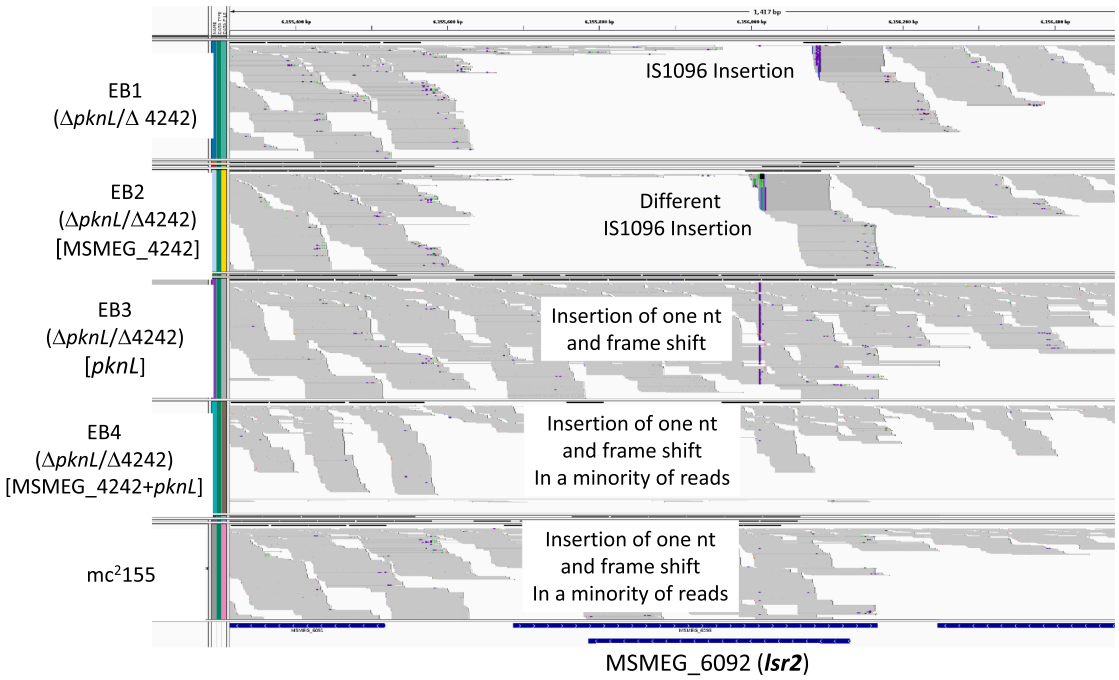

Fig. 3. RNA-seq reads in the region of *lsr2* (MSMEG_6092): EB1 has an IS1096 insertion eliminating *lsr2* transcription; EB2, has a different IS1096 insertion; EB3, showing insertion of a T that causes a frameshift; EB4, a small minority of reads show the same nucleotide insertion as in EB3; wt mc^{2}155, a small minority of reads show the same nucleotide insertion as in EB3.

substitutions or *IS1096* insertions in *lsr2* occurred at a frequency of nearly 10^{-2}, which is unexpectedly high but perhaps partially explained by the increased transcription of IS*1096* transposase TnpA. The growth rate, bacillary length and rifampicin sensitivity of *lsr2* smooth colony mutants were not previously reported to be different from those of the parent strains, although similar to our smooth strains, they showed increased sliding motility (Colangeli et al., 2007; Arora et al., 2008; Chen et al., 2006). Smooth colony *lsr2* mutant strains also had anomalous lipid species, generally polar lipids identified as GPLs (Colangeli et al., 2007) that were present in greater amounts than in the parent strains (Kocíncová et al., 2008). GPLs have been shown to be essential for sliding motility (Recht et al., 2000). One study (Chen et al., 2006) found that two apolar mycolyl-diacylglycerols (MDAGs) were lost in an mc^{2}155 strain with an insertion in *lsr2*, but a recent study convincingly showed that LOS are produced in *lsr2* mutants(Kolodziej et al., 2021).

Apparently, *M. smegmatis* can have many types of variants. The original ATCC607, from which the transformation competent mc^{2}155 was selected (Snapper et al., 1990), could not form biofilms and had low motility (Etienne et al., 2005), but a strain with an *IS1096* inserted into *lsr2* showed increased production of GPLs, increased motility and could not form biofilms. A similar phenotype was found in strains with IS1096 insertions upstream of *MSMEG_0400*, the first gene of the mps operon, whose encoded enzymes synthesize GPLs, and transcription of this operon was increased. Genome sequencing found that *mc^{2}155* has an IS*1096* insertion into this promoter region(Kocíncová et al., 2008). It was reasoned that Lsr2 negatively regulates the synthesis of GPLs by the *mps* gene cluster (Kocíncová et al., 2008) but the IS*1096* insertions abolished the Lsr2 regulatory site. The RNA-seq studies of the smooth colony mutant EB1, which lacks an intact *lsr2* gene, did not show an increase in the transcription of the genes in the *mps* cluster, perhaps because it is already highly expressed in *mc^{2}155* (Kocíncová et al., 2008) due to the IS*1096* insertion upstream of the *mps* operon that eliminated the Lsr2 binding site.

Our triple mutant EB1 (Δ*pknL*/Δ*MSMEG*_4242/Δ*lsr2*) was shown by MS to have several lipid species that are not present in the parent mc^{2}155, probably LOS-A, possibly LOS-C and perhaps GPLs. It was previously shown that the synthesis of these LOS, which were present in the original *M. smegmatis* ATCC607 but lost in the transformation competent *M. smegmatis* mc^{2}155, depends upon the PKS protein encoded by *MSMEG_4727* (Etienne et al., 2009). In strains EB1, 2 and 3 – the smooth colony mutants with inactivated *lsr2* genes, the transcription of *MSMEG_4727* was several times greater than in the parent strain (Table 3), as previously reported for other *lsr2* mutant strains (Colangeli et al., 2007; Kolodziej et al., 2021). When *MSMEG_4727* was eliminated, the strain regained the rough morphology of the parent mc^{2}155, formed strong biofilms and had reduced motility, although still 50% greater than the original mc^{2}155 progenitor. Similar results were recently reported for another *lsr2* mutant(Kolodziej et al., 2021).

Lsr2 is a two-domain protein composed of an N-terminal dimerization domain and a C-terminal DNA-binding domain. The crystal structure of the truncated N-terminal dimer domain (Summers et al., 2012) revealed an elongated molecule made up of a single four-stranded beta-sheet with two helices on one side. The carboxylate groups of the two Asp35, which are replaced by Alanine in some of the smooth mutants, are completely exposed to the solvent at each extremity (Figure S4). The N-terminal domain can also promote higher-order Lsr2 assemblies, providing a mechanism for the role of Lsr2 in the compaction and physical protection of DNA (Colangeli et al., 2009). Since Asp35 is directly engaged in dimer-dimer electrostatic contacts leading to higher oligomers, the Asp35-Ala substitution might limit the ability of Lsr2 to form these higher-order DNA binding assemblies.

Lsr2 binds to multiple DNA targets, but when phosphorylated by PknB on threonine 112, its ability to bind to DNA is abrogated (Alqaseer et al., 2019). Thus, phosphorylation of Lsr2 would lead to increased expression of the genes it represses, such as *MSMEG_4727* (Kocíncová et al., 2008; Kolodziej et al., 2021). Perhaps PknL can also phosphorylate Lsr2, but as PknL cannot autophosphorylate (Baer et al., 2014), there may be a phosphorylation cascade whereby PknB phosphorylates PknL, which in turn phosphorylates Lsr2 (Fig. 6 A-C). However, there is currently no experimental evidence that PknL can phosphorylate Lsr2, which may only be phosphorylated by PknB (Fig. 6E).

PknL has been shown to phosphorylate the protein encoded by the

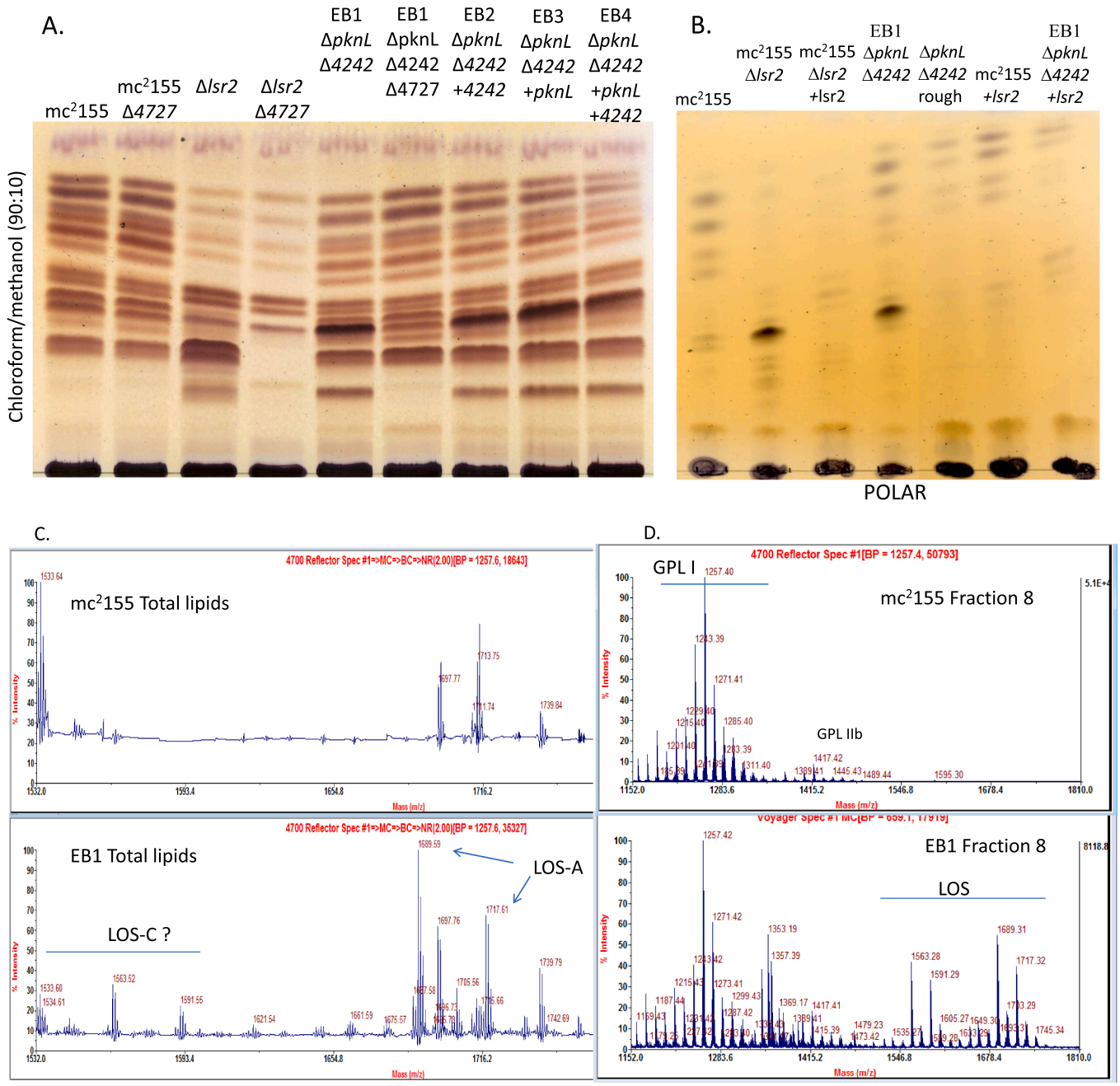

Fig. 4. Thin layer chromatography. Anomalous lipid bands in *lsr2* mutant strains were eliminated either by inactivating the MSMEG_4727 (PKS5) gene (**A**), or complementing with a plasmid containing an intact copy of *lsr2* (**B**). **C.** Mass spectrometry of wt mc^{2}155 and EB1 total lipids, or **D.** fraction 8.

adjacent and divergently transcribed, putative transcriptional regulator Rv2175c, the *M. tuberculosis* equivalent of *MSMEG_4242*, which then loses its ability to bind DNA (Molle and Kremer, 2010). In an alternative model, the unphosphorylated *MSMEG_4242*/Rv2175c represses the expression of LOS and GPL synthesis and the repression is relieved when this transcriptional regulator is phosphorylated by PknL, which in turn is phosphorylated by PknB (Fig. 6D). The phosphorylation of Rv2175c or Lsr2 would abrogate their ability to bind DNA and repress transcription, which would induce the expression of the lipid-producing genes they regulate. This is consistent with other studies showing that phosphorylation by PknB has a negative effect on protein function, which also results in decreased synthesis and transport of mycolates to the envelope (Le et al., 2020; Kolodziej et al., 2021).

An intriguing finding from this study was that strains lacking *pknL* and *MSMEG_4242* accumulate mutations or insertions in *lsr2* at a very high frequency, ~ 10^{-2}. Presumably this is because the lack of PknL somehow causes stress in the bacteria, which is reflected in the increased transcription of *tnpA*, the IS*1096* transposase. The rough colony *pknL/MSMEG_4242* mutants did not show altered lipid bands by TLC but had a reduced sliding motility that was aberrant, jagged and asymmetric (Fig. 2F), as well as weak, delayed formation of biofilms (Fig. 2E), suggesting that PknL is involved with the synthesis of cell envelope components. Other viable *M. smegmatis* variants, including ATCC607, also lack sliding motility but show a much lower frequency of insertions into *lsr2*. However, the very abnormal motility in the rough Δ*pknL*/Δ*MSMEG_4242* mutants may reflect severe, unknown alterations in the cell envelope. Perhaps the LOS or other lipid species produced by *lsr2* inactivation somehow compensate for these undefined defects. It is interesting that in EB4, the Δ*pknL*/Δ*MSMEG_4242* strain with integrated *pknL*/MSMEG_4242, a frameshifting nucleotide deletion was seen in

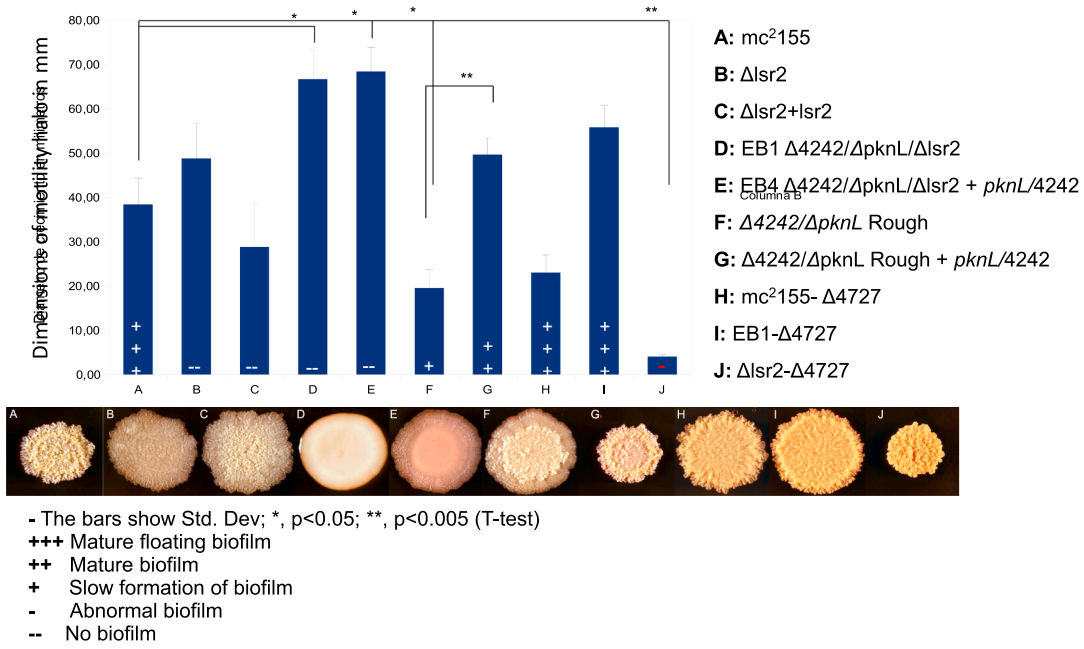

Fig. 5. Summary of colony morphology, biofilm formation and spreading motility. Colony morphology of the strains whose genotypes are shown on the right. The height of the bars in the histogram indicates the average diameter of the sliding motility halos of three independent experiments, with duplicates of each strain in each of the three experiments. One experiment is shown in Fig. 2G. Asterisks (*) indicate a significant difference in the diameter of the halo: *, $P < 0.05$; **, $P < 0.005$ The biofilms formed by each strain are indicated by +'s or –'s according to the key shown below the colonies, based on three experiments, each with duplicates, as in Fig. 2F.

very few reads. The EB4 mutant was originally smooth but changed its phenotype with passaging and the RNA-seq was performed after many passages. This could indicate that the defect that led to the *lsr2* mutations was alleviated by the integrated complementing genes, or alternatively, possible contamination with the parent strain. This same frameshifting mutation was seen in reads from EB3, in a minority of reads in the parent strain and was even present in three reads from EB1.

The phenotypic changes produced by the inactivation of *lsr2* suggest a phase change from a strain that forms biofilms and has moderate motility, to one that does not form biofilms, has high motility and is therefore more likely to spread rather than attach to a surface. The lipid components of the outer cell envelope seem to spontaneously vary in *M. smegmatis*, giving rise to many variants (Kocíncová et al., 2008), which may be a mechanism for survival in different environments (Kolodziej et al., 2021) (Wang et al., 2008). In *M. abscessus*, the rough colony strains lack GPLs present in smooth morphotypes and are more virulent in animal models, but the smooth *M. abscessus* variants are perhaps better suited for survival in environmental niches(Roux et al., 2016; Bernut et al., 2014; Howard et al., 2006). In contrast with *M. smegmatis*, though, deletion of *lsr2* in *M. abscessus* has no effect on the GPL profile, at least under laboratory growth conditions (Le Moigne et al., 2019). Similarly, it was recently suggested that rough morphotypes of *M. kansasii* might be an adaptation favorable for human pathogenicity (Luo et al., 2021). Perhaps the smooth *M. canettii,* or its recent ancestors, existed in an environmental niche but lost their LOS when they evolved into the rough, aggregative pathogen *M. tuberculosis* (Boritsch et al., 2016), which is not known to grow outside of mammalian hosts. Although we do not know exactly how PknL functions, nor exactly which lipid components determine sliding motility, biofilm formation and colony morphotype, this study suggests that both Lsr2 and PknL are involved in regulating components of the outer cell wall of *M. smegmatis*, but this regulation seems complex. Likely the conserved transcriptional regulator adjacent to PknL (*MSMEG_4242*/Rv2175c), as well as additional regulators such as other nucleoid-associated proteins (Ghosh et al., 2013) or other STPK could also be involved in the synthesis(Le et al., 2020) and export(Le et al., 2020; Pérez et al., 2006; Melly et al., 2021) of the components of the cell envelope that determine these complex phenotypes.

4. Methods

4.1. Construction and selection of mutants.

Vector pUC19, modified to eliminate the BamHI site, was used to clone a 4450 bp fragment amplified from a boiled lysate of *mc²155* with primers PknLXbaIFw and PknLXbaIRv (Table S1). This fragment included *MSMEG_4242*, *MSMEG_4243* (*pknL*) and 1500 pb on either side of these genes. This construct was then cut with BamHI to eliminate the 5′ end of *MSMEG_4242*, the intergenic region and half of *MSMEG_4243* (*pknL*), including the kinase motif, and then religated with a kanamycin resistance cassette cut from pUC4K with BamHI. The entire insert, with the Kan cassette, was cut with XbaI and ligated into pPR27.

The pPR27-Δ*pknL/ΔMsmeg4242*::kan^R construct and control vector pPR27 and modified pPR17-pJV53 were electroporated into *M. smegmatis* mc²155, and also *M. smegmatis* mc²155 strains containing chromosomally integrated pYUB412int plasmids with *MSMEG_4242*, *MSMEG_4243*(*pknL*), or both genes. The electroporated strains were then plated onto 7H10-OAD (Oleic Acid, Albumin Dextrose) with kanamycin and gentamycin and incubated at 32 °C. for 4–5 days(Pelicic et al., 1997). Colonies from these plates were inoculated into 5 ml of 7H9-OAD-kanamycin (25 μg/ml) and grown until saturation for 4 days at 32 °C. From these liquid cultures, 5 ul (first expt.) or 100 ul (second expt.) were plated onto 7H10-OAD-kan (25 μg/ml) with 10% sucrose and grown at 39 °C. until colonies appeared (10 – 15 days). All of the colonies that appeared were grown in 7H9-OAD-Kan (25 μg/ml) at 39° C (first experiment) or 37 °C (second experiment), and the second crossover event was confirmed by the inability to grow on 7H10-OAD plates with gentamycin 5 μg/ml.

To construct knockouts of single genes, first plasmid pUC119 was cut with PstI and filled-in with Klenow (NEB) to make pUC2P, and separately the HindIII site was similarly eliminated to make pUC2H. Two 1500 bp fragments, one containing *MSMEG_4241* and *MSMEG_4243*

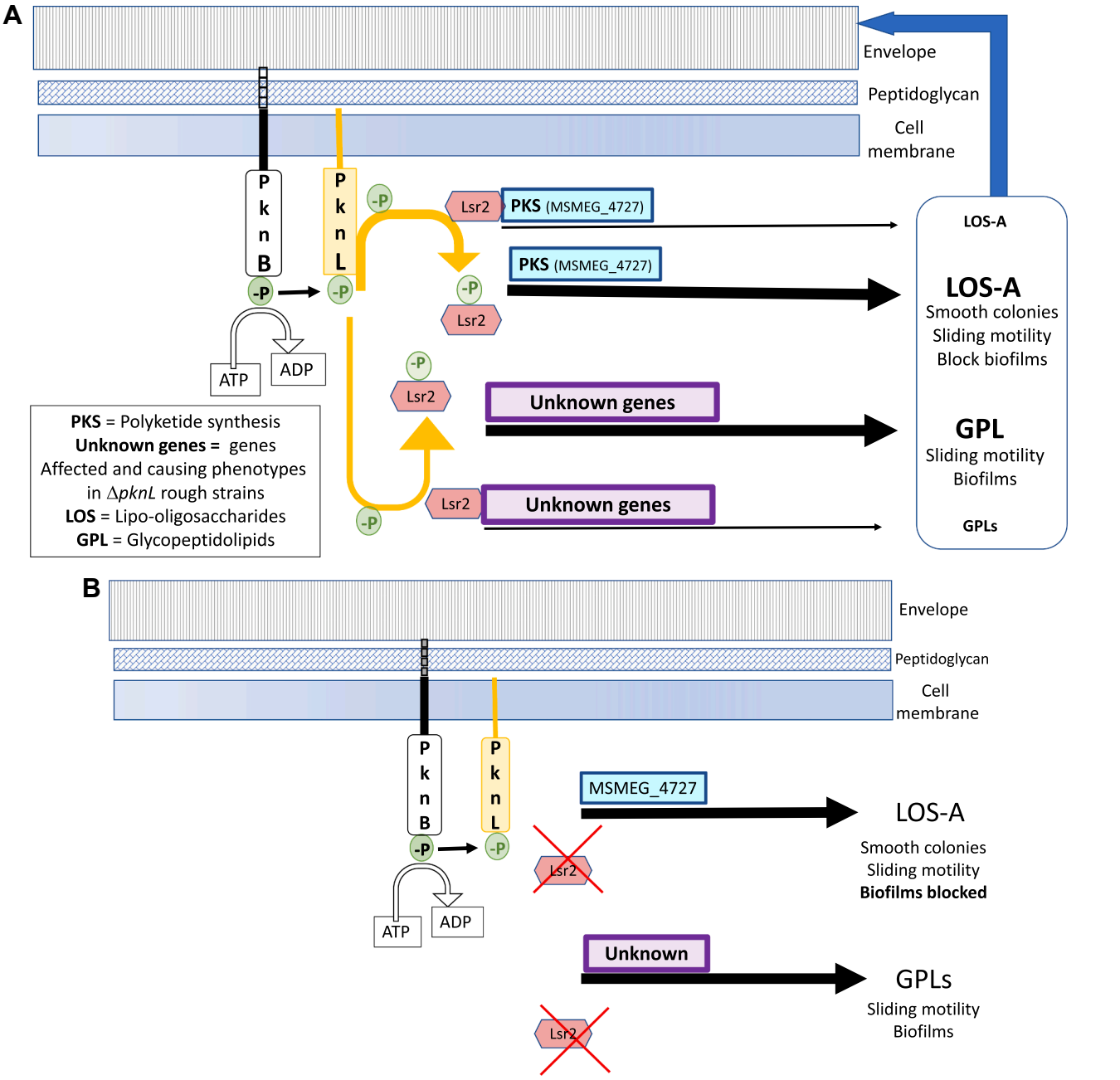

Fig. 6. Hypothetical schemes of how PknL might function to produce the phenotype seen in the mutant strains. While the loss of *lsr2* is responsible for several of the phenotypes in the EB series smooth mutant strains, the rough mutants have altered motility and biofilm formation despite having an intact *lsr2* gene. The gene or genes responsible for the phenotypes of the rough strains are unknown. A. PknB phosphorylates PknL and PknL phosphorylates Lsr2, which abolishes its ability to bind DNA and thus relieves the repression of LOS-A and GPL synthesis. B. In an *lsr2* mutated strain there is unrepressed synthesis of LOS-A and GPLs PknL phosphorylates Lsr2.C. In a *pknL* knockout, the unphosphorylated Lsr2 represses LOS & GPL synthesis. D. In an alternative scheme, PknB phosphorylates PknL (MSMEG_4243) and PknL phosphorylates the putative transcriptional regulator encoded by the adjacent gene MSMEG_4242, which then loses its ability to bind DNA and repress gene transcription, resulting in the synthesis of GPL and LOS-A. E.Another possibility is that PknB phosphorylates Lsr2 directly, without PknL serving as a phosphorylation cascade intermediate.

(*pknL*) and the other *MSMEG_4242* and *MSMEG_4244* (Fig. 1Ba) were amplified from an *M. smegmatis* boiled lysate with primers 1KOFw4242-1KORv4242, 2KOFw4242-2KORv4242 and 1KOFw4243-1KORv4243, 2KOFw4243-2KORv4243 (Table S1). The amplified fragments containing *MSMEG_4242* were cut with PstI, eliminating most of this gene, then religated and inserted into the XbaI site of pUC3P to make pUCKO4242 (Fig. 1Bb). The amplified fragments containing *MSMEG_4243*(*pknL*), were cut with HindIII, religated and then inserted into the XbaI site of pUC2H to make pUCKO4243 (Fig. 1Bc). The *aph* kanamycin resistance cassette was then inserted into the PstI site of pUCK04242 and the HindIII site of pUCK04243 (Fig. 1B d & e). The plasmids were transformed into *E. coli* XL1Blue and plated on agar with kanamycin and carbenicillin. The fragments *MSMEG_4242*::Kan^R and MSMEG_KO4243::Kan^R were then cut from the pUC plasmids and ligated into vector pPR27 and electroporated into *M. smegmatis* mc^{2}155 for allelic exchange, as described above.

The *lsr2* mutant strain was the kind gift of Roberto Colangeli, along with *lsr2* containing, complementing plasmid pMP161.

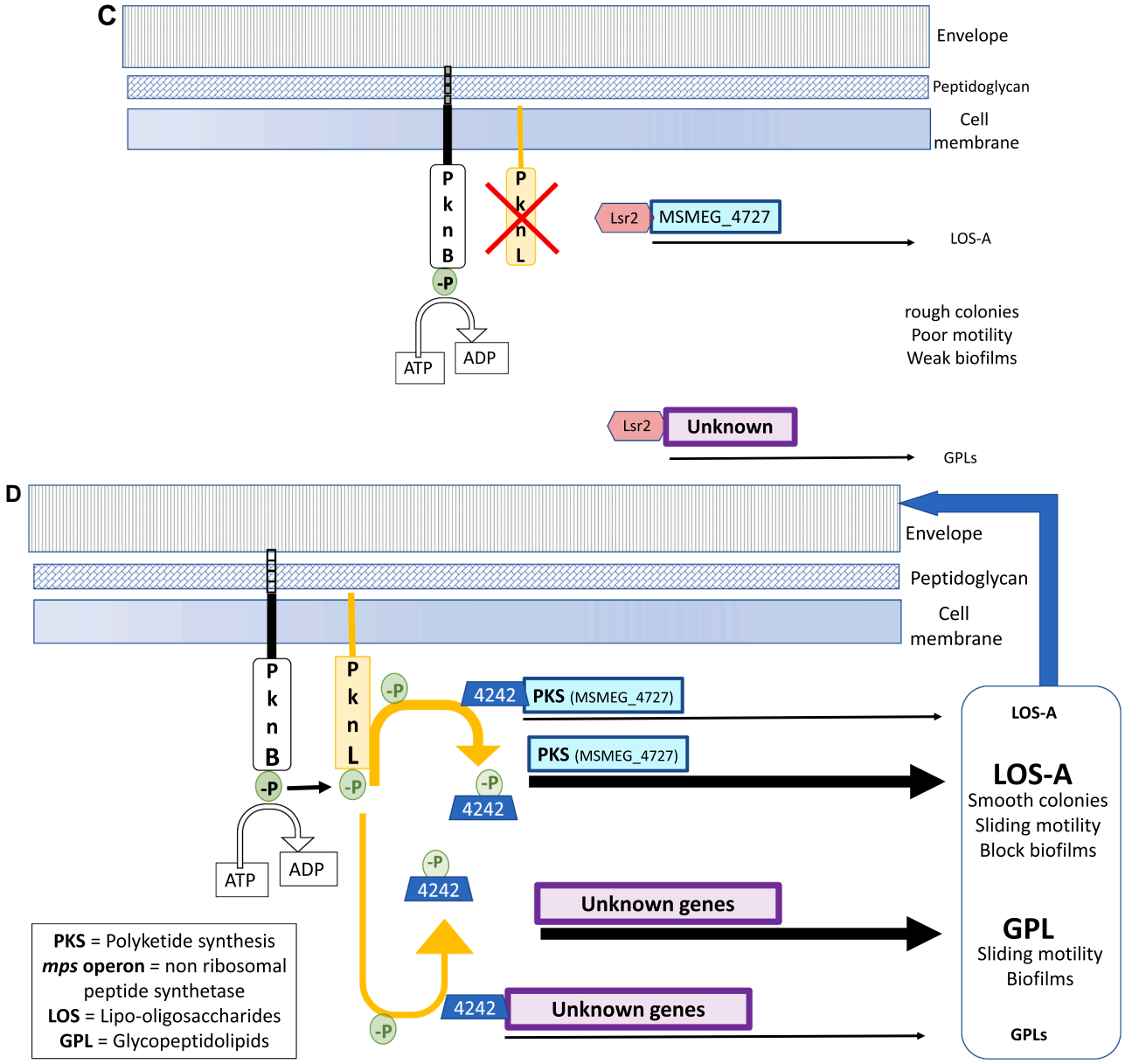

Fig. 6. (*continued*).

4.2. Confirmation of mutants.

Gentamycin sensitive colonies were grown in 7H9-OAD-Kan and 1 ml of culture was centrifuged, resuspended in 150 ul sterile distilled water and boiled for 10 min. From this boiled lysate, 10 ul were used in a PCR amplification with primers Msmeg_4242pknLsmeg412Fw y pknLsmeg412Rv (Table S1), and the product was sequenced in CeSAAN (IVIC, Caracas, Venezuela) and subjected to restriction analysis. The elimination of the two genes was also subsequently confirmed by RNA-seq.

4.3. Cloning of complementing integrative plasmids.

Vector pYUB412int was transformed into *E.coli* K12 ER2925 (*dam*$^-$) in order to use the *BclI* cloning site, and grown in LB broth with carbenicillin 50 ug/ml. The amplified fragments containing *MSMEG_4242*, *MSMEG_4243*(*pknL*), or both genes (Table S1) were ligated into the pYUBint vector using the *BclI*, or *PacI* sites, and then electroporated into mc^{2}155 (Snapper et al., 1990) and plated onto 7H10-OAD-Hygromicin 50 μg/ml, and the presence of the inserts verified by PCR amplification and restriction digests.

4.4. Ziehl-Neelsen staining

Ziehl-Neelsen staining was performed using the traditional method. Slides spread with 10 μl of a bacterial suspension were fixed over a flame. They were then covered with phenol fucsin, heated over a flame three times during a period of ten minutes, and then washed with distilled water. The slides were then covered with acid alcohol for 3 min and again washed with distilled water. Finally, the slides were covered with methylene blue for one minute, washed, left to air dry and examined with a 100X objective microscope.

4.5. Measurements of bacilli length.

From exponential phase cultures (DO_{600} = 0,8–1), 10 μl were placed on glass microscope slides and air dried. After adding 2 μl of glycerol, the slides were examined with a Nikon E-600 microscope using a 100X oil

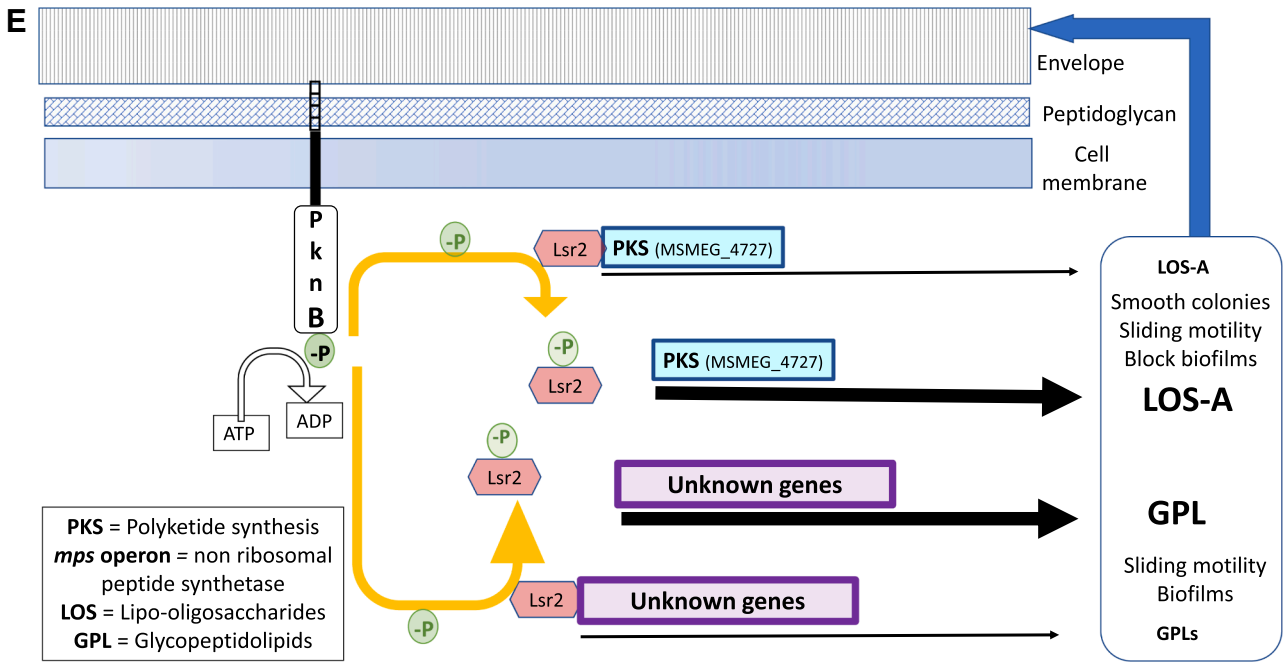

Fig. 6. (*continued*).

immersion objective. DIC (Differential Interference Contrast) images were taken, blinded to strain identification, with a digital Hamamatsu camera using the Methamorph program. The lengths of 50 bacilli of each strain were measured with Image-J software.

4.6. Motility assay.

Colonies were inoculated into 7H9 with 10% OAD and 0.05% Tween 80 and grown to mid log phase ($D.O_{600nm} = 0.4 – 0.6$). A toothpick was dipped into the culture, excess drops were allowed to fall off, and it was stabbed into the center of a Petri dish containing 7H9 media without glycerol and 0.3% agarose. The diameter of the motility halo was measured after 2 days of incubation at 37 °C.

4.7. Biofilm assays

Biofilm formation was assessed by inoculating 20 ul of a bacterial culture (OD_{600}, 0.8 to 1.0) onto the wells of a 6 well plate, each containing 4 ml of M63 salts supplemented with 10% glucose, 1 mM $CaCl_2$ and 1 mM $MgSO_4$ and then incubated without shaking at 30 °C for 5 days.

4.8. Determination of rifampicin sensitivity

The strains were grown in 7H9-OAD at 37 °C. until reaching log phase (1–5 × 10^8 CFU/ml), diluted 1:100 and then 10 ul of the dilution was inoculated onto 2 mls of 7H10-OAD with rifampicin 32 or 64 μg/mL in a 24 well plate and incubated at 37 °C for 3 to 5 days until confluent growth was observed. Each strain was tested in triplicate.

4.9. RNA-seq analysis

The strains were grown in 7H9-OADC at 37 °C, RNA was isolated, reverse transcribed and sequenced as previously described (Solans et al., 2014). Illumina reads were mapped against the *M. smegmatis* mc^2155 reference sequence (NCBI RefSeq: NC_008596.1) with bowtie2 (Langmead and Salzberg, 2012) v.2.0.0-beta7. Gene counts (based on the NC_008596.1 annotation) were obtained with *htseq-count* tool (https://htseq.readthedocs.io/en/release_0.11.1/count.html). To minimize count bias from overlapping genes, overlapping gene regions (except for nested genes) were excluded and the option '-m intersection-strict' was used. Differential gene expression analysis was done with the DESeq package (Anders and Huber, 2010) v.1.12.1. Alignments were visualized in the IGV viewer(Thorvaldsdottir et al., 2013). The RNA-seq data is available under BioProject reference PRJNA735510.

To look for new IS*1096* insertions, the transcriptome of each mutant was assembled *de novo* using SPAdes v.3.15.2 with the "–rna" option (Bushmanova et al., 2019). Transcripts containing the IS1096 sequence were identified using BLASTn and the IS*1096*′ flanking sequences were blasted against the mc^2155 reference genome to infer their location. IS*1096* insertion sites from the transcriptomes were compared to the known sites in the reference genome (Wang et al., 2008) to determine whether their location corresponded to a known lS*1096* insertion site in the reference genome or constituted a new insertion site unique to the mutant.

4.10. Lipid extractions and (HP)TLC analyses

Bacteria were cultured to Log growth phase in 7H9-OADC, collected by centrifugation and washed twice with PBS. Apolar and polar lipid fractions were extracted from 50 mg of wet-weight bacterial pellet and the polar lipid fraction analysed by thin-layer liquid chromatography as previously described (Besra, 1998). The total extractable lipids were recovered from wet bacterial pellets by three successive extractions using distinct mixtures of $CHCl_3$:CH_3OH (1:2, 1:1 and 2:1, v/v). The fractions were pooled, washed with water and dried. For thin-layer chromatography (TLC) analysis, equivalent weights of total lipid fraction from each strain were spotted on silica gel 60 plates (Merck), which were developed either in $CHCl_3$:CH_3OH (9:1, v/v) or in $CHCl_3$:CH_3OH:H_2O (65:25:4, v/v/v), as indicated. Compounds were revealed by spraying with 0.2% (w/v) anthrone in concentrated H_2SO_4 followed by heating at 100 °C.

The relative abundance of the different types of lipids from each strain was determined by loading a fixed amount (5 μg) of lipid mixture onto a high-performance TLC (HPTLC) silica gel 60 plate (Merck) with a Camag ATS4 apparatus. The plate was developed in appropriate organic solvent mixtures using a Camag ADC2 device and stained by immersion in 10% (w/v) $CuSO_4$ (in H_3PO_4:CH_3OH:H_2O, 8:5:87, v/v/v) with a

Camag CID3 apparatus, followed by heating at 150 °C for 20 min. Lipids were quantified by absorption measurement at 400 nm with a Camag Scanner 3 device using Wincats software.

4.11. MALDI-TOF MS and NMR spectroscopy

Matrix assisted laser desorption ionization-time of flight mass spectrometry (MALDI-TOF MS) and MS/MS analyses were performed in the positive ionization and reflectron mode, using the 5800 MALDI-TOF/TOF Analyzer (Applied Biosystems/ABsciex) equipped with a Nd:YAG laser (349 nm wavelength). MS and MS/MS spectra were acquired with a total of 2,500 shots at a fixed laser intensity of 4,000 (instrument-specific units) and 400-Hz pulse rate for MS, and a total of 5000 shots at a fixed laser intensity of 6000 (instrument-specific units) and 1000-Hz pulse rate for MS/MS. For MS/MS data acquisition, the fragmentation of selected precursor ions was performed at a collision energy of 1 kV using air as collision gas. Lipid samples were dissolved in chloroform and were directly spotted onto the target plate as 0.5 μl droplets, followed by the addition of 0.5 μl of matrix solution {10 mg/ml of 2,5-dihydroxybenzoic acid (Sigma-Aldrich) in $CHCl_3/CH_3OH$ (1:1, v/v)}. Samples were allowed to crystallize at room temperature. MS data were acquired using the instrument default calibration.

CRediT authorship contribution statement

Estalina Báez-Ramírez: Conceptualization, Methodology, Formal analysis, Investigation, Visualization, Writing - review & editing. **Luis Querales:** Conceptualization, Methodology, Formal analysis, Investigation, Visualization. **Carlos Andres Aranaga:** Conceptualization, Methodology, Formal analysis, Investigation, Visualization, Writing - review & editing. **Gustavo López:** Conceptualization, Methodology, Formal analysis, Investigation, Visualization. **Elba Guerrero:** Conceptualization, Methodology, Formal analysis, Investigation, Visualization. **Laurent Kremer:** Conceptualization, Methodology, Resources, Supervision, Funding acquisition, Visualization, Supervision, Writing - review & editing. **Séverine Carrère-Kremer:** Methodology, Investigation. **Albertus Viljoen:** Methodology, Formal analysis, Investigation, Visualization, Writing - original draft, Writing - review & editing. **Mamadou Daffé:** Methodology, Formal analysis, Resources, Visualization, Supervision. **Françoise Laval:** Methodology, Formal analysis, Investigation, Visualization. **Stewart Cole:** Resources, Supervision, Funding acquisition, Writing - review & editing. **Andrej Benjak:** Methodology, Software, Formal analysis, Investigation, Visualization, Writing - original draft, Writing - review & editing. **Pedro Alzari:** Formal analysis, Funding acquisition, Writing - original draft, Writing - review & editing. **Gwenaëlle André-Leroux:** Methodology, Investigation. **William R. Jacobs Jr.:** Resources, Supervision, Funding acquisition, Writing - review & editing. **Catherine Vilcheze:** Methodology, Formal analysis, Investigation, Writing - review & editing. **Howard E. Takiff:** Conceptualization, Methodology, Formal analysis, Resources, Visualization, Supervision, Investigation, Data curation, Funding acquisition, Writing - original draft, Writing - review & editing, Project administration.

Declaration of Competing Interest

The authors declare that they have no known competing financial interests or personal relationships that could have appeared to influence the work reported in this paper.

Acknowledgements

The authors thank Roberto Colangeli for the gift of his lsr2 mutant strain and complementing plasmid pMP161 and Anne Marie Wehenkel, Tristan Wagner and Marco Bellinzoni for helpful discussions. The authors also thank IVIC's Department of Scientific Photography, especially Winston Castillo, Brian Dominguez and Jorge Rivas for their patience and expertise in documenting the phenotypes of the mutant strains, as well as Lorenzo Alamo of the Department of Biología Estructural and Victor Salazar of the Centro de Bioquimica y Biofísica for help with the microscopic analysis. The work for this project was supported by Ecos Nord project PI-200000300 (to P.A. & H.T.), Misión Ciencia Project, "Identificación y caracterización de blancos especificos para nuevos fármacos contra enfermedades transmisibles" (to H.T.) , Fonacit Project S1-2001000853 (to H.T.), the Sanming Project of Medicine in Shenzhen (grant number SZSM201603029), the Swiss National Science Foundation, grant number 31003A_162641 (to STC), NIH, NIAID Grant # R01AI026170 (to W.R.J. Jr.), Fondation pour la Recherche Médicale (FRM) (DEQ20150331719) (to L.K.) This manuscript recalls fond memories of our colleague and friend Gustavo López, aka www.Gustavo, the LGM information source.

Appendix A. Supplementary data

Supplementary data to this article can be found online at https://doi.org/10.1016/j.tcsw.2021.100060.

References

Molle V, Kremer L. 2010. Division and cell envelope regulation by Ser/Thr phosphorylation: Mycobacterium shows the way. Molecular microbiology 75:1064-77.

Kang CM, Abbott DW, Park ST, Dascher CC, Cantley LC, Husson RN. 2005. The Mycobacterium tuberculosis serine/threonine kinases PknA and PknB: substrate identification and regulation of cell shape. Genes Dev 19:1692-704.

Narayan, A., Sachdeva, P., Sharma, K., Saini, A.K., Tyagi, A.K., Singh, Y., 2007. Serine threonine protein kinases of mycobacterial genus: phylogeny to function. Physiological genomics 29 (1), 66–75.

Wehenkel, A., Bellinzoni, M., Graña, M., Duran, R., Villarino, A., Fernandez, P., Andre-Leroux, G., England, P., Takiff, H., Cerveñansky, C., Cole, S.T., Alzari, P.M., 2008. Mycobacterial Ser/Thr protein kinases and phosphatases: physiological roles and therapeutic potential. Biochimica et biophysica acta 1784 (1), 193–202.

Refaya, A.K., Sharma, D., Kumar, V., Bisht, D., Narayanan, S., 2016. A Serine/threonine kinase PknL, is involved in the adaptive response of Mycobacterium tuberculosis. Microbiol Res 190, 1–11.

Naz, S., Singh, Y., Nandicoori, V.K., 2021. Deletion of serine/threonine-protein kinase pknL from Mycobacterium tuberculosis reduces the efficacy of isoniazid and ethambutol. Tuberculosis (Edinb) 128, 102066.

Canova, M.J., Veyron-Churlet, R., Zanella-Cleon, I., Cohen-Gonsaud, M., Cozzone, A.J., Becchi, M., Kremer, L., Molle, V., 2008. The Mycobacterium tuberculosis serine/threonine kinase PknL phosphorylates Rv2175c: mass spectrometric profiling of the activation loop phosphorylation sites and their role in the recruitment of Rv2175c. Proteomics 8 (3), 521–533.

Cohen-Gonsaud, M., Barthe, P., Canova, M.J., Stagier-Simon, C., Kremer, L., Roumestand, C., Molle, V., 2009. The Mycobacterium tuberculosis Ser/Thr kinase substrate Rv2175c is a DNA-binding protein regulated by phosphorylation. The Journal of biological chemistry 284 (29), 19290–19300.

Av-Gay, Y., Everett, M., 2000. The eukaryotic-like Ser/Thr protein kinases of Mycobacterium tuberculosis. Trends Microbiol 8 (5), 238–244.

Bellinzoni, M., Wehenkel, A.M., Durán, R., Alzari, P.M., 2019. Novel mechanistic insights into physiological signaling pathways mediated by mycobacterial Ser/Thr protein kinases. Microbes Infect 21 (5-6), 222–229.

Baer, C.E., Iavarone, A.T., Alber, T., Sassetti, C.M., 2014. Biochemical and spatial coincidence in the provisional Ser/Thr protein kinase interaction network of Mycobacterium tuberculosis. J Biol Chem 289 (30), 20422–20433.

Schultz C, Niebisch A, Schwaiger A, Viets U, Metzger S, Bramkamp M, Bott M. 2009. Genetic and biochemical analysis of the serine/threonine protein kinases PknA, PknB, PknG and PknL of Corynebacterium glutamicum: evidence for non-essentiality and for phosphorylation of OdhI and FtsZ by multiple kinases. Molecular microbiology 74:724-41.

Kocíncová, D., Singh, A.K., Beretti, J.-L., Ren, H., Euphrasie, D., Liu, J., Daffé, M., Etienne, G., Reyrat, J.-M., 2008. Spontaneous transposition of IS1096 or ISMsm3 leads to glycopeptidolipid overproduction and affects surface properties in Mycobacterium smegmatis. Tuberculosis (Edinb) 88 (5), 390–398.

Recht, J., Kolter, R., 2001. Glycopeptidolipid acetylation affects sliding motility and biofilm formation in Mycobacterium smegmatis. J Bacteriol 183 (19), 5718–5724.

Chen JM, Ren H, Shaw JE, Wang YJ, Li M, Leung AS, Tran V, Berbenetz NM, Kocincova D, Yip CM, Reyrat JM, Liu J. 2008. Lsr2 of Mycobacterium tuberculosis is a DNA-bridging protein. Nucleic Acids Res 36:2123-35.

Gordon, B.R.G., Li, Y., Wang, L., Sintsova, A., van Bakel, H., Tian, S., Navarre, W.W., Xia, B., Liu, J., 2010. Lsr2 is a nucleoid-associated protein that targets AT-rich sequences and virulence genes in Mycobacterium tuberculosis. Proc Natl Acad Sci U S A 107 (11), 5154–5159.

Etienne, G., Laval, F., Villeneuve, C., Dinadayala, P., Abouwarda, A., Zerbib, D., Galamba, A., Daffe, M., 2005. The cell envelope structure and properties of

Mycobacterium smegmatis mc(2)155: is there a clue for the unique transformability of the strain? Microbiology (Reading) 151, 2075–2086.
Etienne G, Malaga W, Laval F, Lemassu A, Guilhot C, Daffe M. 2009. Identification of the polyketide synthase involved in the biosynthesis of the surface-exposed lipooligosaccharides in mycobacteria. J Bacteriol 191:2613-21.
Colangeli R, Helb D, Vilcheze C, Hazbon MH, Lee CG, Safi H, Sayers B, Sardone I, Jones MB, Fleischmann RD, Peterson SN, Jacobs WR, Jr., Alland D. 2007. Transcriptional regulation of multi-drug tolerance and antibiotic-induced responses by the histone-like protein Lsr2 in M. tuberculosis. PLoS Pathog 3:e87.
Boritsch, E.C., Frigui, W., Cascioferro, A., Malaga, W., Etienne, G., Laval, F., Pawlik, A., Le Chevalier, F., Orgeur, M., Ma, L., Bouchier, C., Stinear, T.P., Supply, P., Majlessi, L., Daffe, M., Guilhot, C., Brosch, R., 2016. pks5-recombination-mediated surface remodelling in Mycobacterium tuberculosis emergence. Nat Microbiol 1, 15019.
Kolodziej M, Lebkowski T, Plocinski P, Holowka J, Pasciak M, Wojtas B, Bury K, Konieczny I, Dziadek J, Zakrzewska-Czerwinska J. 20Lsr2 and Its Novel Paralogue Mediate the Adjustment of Mycobacterium smegmatis to Unfavorable Environmental Conditions. mSphere 6.
Le, N.-H., Locard-Paulet, M., Stella, A., Tomas, N., Molle, V., Burlet-Schiltz, O., Daffé, M., Marrakchi, H., 2020. The protein kinase PknB negatively regulates biosynthesis and trafficking of mycolic acids in mycobacteria. J Lipid Res 61 (8), 1180–1191.
Zeng, J., Platig, J., Cheng, T.Y., Ahmed, S., Skaf, Y., Potluri, L.P., Schwartz, D., Steen, H., Moody, D.B., Husson, R.N., 2020. Protein kinases PknA and PknB independently and coordinately regulate essential Mycobacterium tuberculosis physiologies and antimicrobial susceptibility. PLoS Pathog 16, e1008452.
Kolodziej, M., Trojanowski, D., Bury, K., Holowka, J., Matysik, W., Kakolewska, H., Feddersen, H., Giacomelli, G., Konieczny, I., Bramkamp, M., Zakrzewska-Czerwinska, J., 2021. Lsr2, a nucleoid-associated protein influencing mycobacterial cell cycle. Sci Rep 11, 2910.
Alqaseer, K., Turapov, O., Barthe, P., Jagatia, H., De Visch, A., Roumestand, C., Wegrzyn, M., Bartek, I.L., Voskuil, M.I., O'Hare, H.M., Ajuh, P., Bottrill, A.R., Witney, A.A., Cohen-Gonsaud, M., Waddell, S.J., Mukamolova, G.V., 2019. Protein kinase B controls Mycobacterium tuberculosis growth via phosphorylation of the transcriptional regulator Lsr2 at threonine 112. Mol Microbiol 112 (6), 1847–1862.
Arora, K., Whiteford, D.C., Lau-Bonilla, D., Davitt, C.M., Dahl, J.L., 2008. Inactivation of lsr2 results in a hypermotile phenotype in Mycobacterium smegmatis. J Bacteriol 190 (12), 4291–4300.
Chen, J.M., German, G.J., Alexander, D.C., Ren, H., Tan, T., Liu, J., 2006. Roles of Lsr2 in colony morphology and biofilm formation of Mycobacterium smegmatis. J Bacteriol 188 (2), 633–641.
Recht, J., Martínez, Asunción, Torello, S., Kolter, R., 2000. Genetic analysis of sliding motility in Mycobacterium smegmatis. J Bacteriol 182 (15), 4348–4351.
Snapper, S.B., Melton, R.E., Mustafa, S., Kieser, T., Jr, W.R.J., 1990. Isolation and characterization of efficient plasmid transformation mutants of Mycobacterium smegmatis. Mol Microbiol 4 (11), 1911–1919.
Summers, E.L., Meindl, K., Uson, I., Mitra, A.K., Radjainia, M., Colangeli, R., Alland, D., Arcus, V.L., 2012. The structure of the oligomerization domain of Lsr2 from Mycobacterium tuberculosis reveals a mechanism for chromosome organization and protection. PLoS One 7, e38542.
Colangeli, R., Haq, A., Arcus, V.L., Summers, E., Magliozzo, R.S., McBride, A., Mitra, A. K., Radjainia, M., Khajo, A., Jacobs, W.R., Salgame, P., Alland, D., 2009. The multifunctional histone-like protein Lsr2 protects mycobacteria against reactive oxygen intermediates. Proc Natl Acad Sci U S A 106 (11), 4414–4418.
Wang, X.-M., Galamba, A., Warner, D.F., Soetaert, K., Merkel, J.S., Kalai, M., Bifani, P., Lefèvre, P., Mizrahi, V., Content, J., 2008. IS1096-mediated DNA rearrangements play a key role in genome evolution of Mycobacterium smegmatis. Tuberculosis (Edinb) 88 (5), 399–409.
Roux, A.L., Viljoen, A., Bah, A., Simeone, R., Bernut, A., Laencina, L., Deramaudt, T., Rottman, M., Gaillard, J.L., Majlessi, L., Brosch, R., Girard-Misguich, F., Vergne, I., de Chastellier, C., Kremer, L., Herrmann, J.L., 2016. The distinct fate of smooth and rough Mycobacterium abscessus variants inside macrophages. Open Biol 6.
Bernut, A., Herrmann, J.L., Kissa, K., Dubremetz, J.F., Gaillard, J.L., Lutfalla, G., Kremer, L., 2014. Mycobacterium abscessus cording prevents phagocytosis and promotes abscess formation. Proc Natl Acad Sci U S A 111, E943–52.
Howard, S.T., Rhoades, E., Recht, J., Pang, X., Alsup, A., Kolter, R., Lyons, C.R., Byrd, T. F., 2006. Spontaneous reversion of Mycobacterium abscessus from a smooth to a rough morphotype is associated with reduced expression of glycopeptidolipid and reacquisition of an invasive phenotype. Microbiology (Reading) 152, 1581–1590.
Le Moigne, V., Bernut, A., Cortes, M., Viljoen, A., Dupont, C., Pawlik, A., Gaillard, J.L., Misguich, F., Cremazy, F., Kremer, L., Herrmann, J.L., 2019. Lsr2 Is an Important Determinant of Intracellular Growth and Virulence in Mycobacterium abscessus. Front Microbiol 10, 905.
Luo, T., Xu, P., Zhang, Y., Porter, J.L., Ghanem, M., Liu, Q., Jiang, Y., Li, J., Miao, Q., Hu, B., Howden, B.P., Fyfe, J.A.M., Globan, M., He, W., He, P., Wang, Y., Liu, H., Takiff, H.E., Zhao, Y., Chen, X., Pan, Q., Behr, M.A., Stinear, T.P., Gao, Q., 2021. Population genomics provides insights into the evolution and adaptation to humans of the waterborne pathogen Mycobacterium kansasii. Nat Commun 12, 2491.
Ghosh, S., Indi, S.S., Nagaraja, V., 2013. Regulation of lipid biosynthesis, sliding motility, and biofilm formation by a membrane-anchored nucleoid-associated protein of Mycobacterium tuberculosis. J Bacteriol 195 (8), 1769–1778.
Pérez, J., Garcia, R., Bach, H., de Waard, J.H., Jacobs, W.R., Av-Gay, Y., Bubis, J., Takiff, H.E., 2006. Mycobacterium tuberculosis transporter MmpL7 is a potential substrate for kinase PknD. Biochemical and biophysical research communications 348 (1), 6–12.
Melly, G.C., Stokas, H., Davidson, P.M., Roma, J.S., Rhodes, H.L., Purdy, G.E., 2021. Identification of residues important for M. tuberculosis MmpL11 function reveals that function is modulated by phosphorylation in the C-terminal domain. Mol Microbiol 115, 208–221.
Solans, L., Gonzalo-Asensio, J., Sala, C., Benjak, A., Uplekar, S., Rougemont, J., Guilhot, C., Malaga, W., Martin, C., Cole, S.T., 2014. The PhoP-dependent ncRNA Mcr7 modulates the TAT secretion system in Mycobacterium tuberculosis. PLoS Pathog 10, e1004183.
Langmead, B., Salzberg, S.L., 2012. Fast gapped-read alignment with Bowtie 2. Nat Methods 9 (4), 357–359.
Anders, S., Huber, W., 2010. Differential expression analysis for sequence count data. Genome Biol 11, R106.
Thorvaldsdottir, H., Robinson, J.T., Mesirov, J.P., 2013. Integrative Genomics Viewer (IGV): high-performance genomics data visualization and exploration. Brief Bioinform 14 (2), 178–192.
Bushmanova, E., Antipov, D., Lapidus, A., Prjibelski, A.D., 2019. rnaSPAdes: a de novo transcriptome assembler and its application to RNA-Seq data. Gigascience 8.
Besra GS. 1998. Preparation of Cell-Wall Fractions from Mycobacteria, p 91-108, Mycobacteria Protocols vol 101. Humana Press.
Pelicic, V., Jackson, M., Reyrat, J.-M., Jacobs, W.R., Gicquel, B., Guilhot, C., 1997. Efficient allelic exchange and transposon mutagenesis in Mycobacterium tuberculosis. Proc Natl Acad Sci U S A 94 (20), 10955–10960.